FABRICATION OF FIBER METAL LAMINATED COMPOSITES BY RESIN INFUSION TECHNIQUE USING METALLIC LAYERS WITH MODIFIED SURFACE

A THESIS SUBMITTED TO
THE GRADUATE SCHOOL OF NATURAL AND APPLIED SCIENCES
OF
MIDDLE EAST TECHNICAL UNIVERSITY

BY

GÜNEY DALOĞLU

IN PARTIAL FULFILLMENT OF THE REQUIREMENTS
FOR
THE DEGREE OF MASTER OF SCICENCE
IN
METALLURGICAL AND MATERIALS ENGINEERING

NOVEMBER 2014

Approval of the thesis:

FABRICATION OF FIBER METAL LAMINATED COMPOSITES BY RESIN INFUSION TECHNIQUE USING METALLIC LAYERS WITH MODIFIED SURFACE

submitted by **GUNEY DALOĞLU** in partial fulfillment of the requirements for the degree of **Master of Science in Metallurgical and Materials Engineering Department, Middle East Technical University** by,

Prof. Dr. Gülbin Dural Ünver _____
Dean, **Graduate School of Natural and Applied Sciences**

Prof. Dr. Cemil Hakan Gür _____
Head of Department, **Metallurgical and Materials Eng.**

Assoc. Prof. Dr. Arcan F. Dericioğlu _____
Supervisor, **Metallurgical and Materials Eng. Dept**., **METU**

Prof. Dr. A. Şakir Bor _____
Co-Supervisor, **Metallurgical and Materials Eng. Dept**., **METU**

Examining Committee Members:

Prof. Dr. Cemil Hakan Gür _____
Metallurgical and Materials Eng. Dept., METU

Assoc. Prof. Dr. Arcan F. Dericioğlu _____
Metallurgical and Materials Eng. Dept., METU

Prof. Dr. A. Şakir Bor _____
Metallurgical and Materials Eng. Dept., METU

Prof. Dr. Cevdet Kaynak _____
Metallurgical and Materials Eng. Dept., METU

Assoc. Prof. Dr. Demirkan Çöker _____
Aerospace Eng. Dept., METU

Date: 21.11.2014

I hereby declare that all information in this document has been obtained and presented in accordance with academic rules and ethical conduct. I also declare that, as required by these rules and conduct, I have fully cited and referenced all material and results that are not original to this work.

Name, Last name: Güney Daloğlu

Signature :

ABSTRACT

FABRICATION OF FIBER METAL LAMINATED COMPOSITES BY RESIN INFUSION TECHNIQUE USING METALLIC LAYERS WITH MODIFIED SURFACE

Daloğlu, Güney
MSc, Department of Metallurgical and Materials Engineering
Supervisor: Assoc. Prof. Dr. Arcan F. Dericioğlu
Co-Supervisor: Prof. Dr. A. Şakir BOR

November 2014, 105 pages

Fiber metal laminated composites are novel materials which have been developed in the last few decades especially for fatigue prone areas within the aircrafts. They consist of metals with modified surfaces and fiber reinforced polymer matrix composites.

Surface modification of metals carries importance because their bonding with fiber-resin matrix needs interdisciplinary knowledge about interface engineering. Surface of the metal substrates must be contaminant and moisture free and void content through interfaces of the final composite must be as low as possible to reach the desired mechanical strength. So, wetting of the liquid/resin and wettability capability of the solid/metal surface must be optimized. Different surface modifications like etching, anodizing, plasma spraying, laser texturing, silane or sol-gel etc. treatments are being used solely or together by industry. Fiber metal laminated composites have been investigated under the scope of etching-anodizing surface pretreatment with adhesive primer and fabricated with prepreg-autoclave manufacturing technique which are long-batch and expensive techniques while they are also hazardous.

Within this study, surface treatments of aluminum 2024 T3 alloy based on sand paper abrasion and γ-glycidoxytrimethoxy silane treatment and fabrication of the fiber metal laminated composites by vacuum infusion manufacturing technique have been studied. The stress-strain and load-displacement relations and interface on both sides of composites have been investigated in relation with the surface roughness-contact angle-spreading capability controlled by the surface treatments applied. Achieved results have shown that vacuum infusion is a successful alternative technique for the fabrication of fiber metal laminated composites.

Keywords: Fiber metal laminated composite, vacuum infusion, γ-glycidoxytrimethoxy silane, 2024 T3 aluminum alloy, surface pretreatment, roughness, contact angle, spreading.

ÖZ

REÇİNE İNFÜZYONU TEKNİĞİ İLE YÜZEYİ MODİFİYE EDİLMİŞ METALİK KATMANLAR KULLANILARAK FİBER-METAL KATMANLI KOMPOZİT MALZEME ÜRETİMİ

Daloğlu, Güney
Yüksek Lisans, Metalurji ve Malzeme Mühendisliği Bölümü
Tez Yöneticisi: Doç. Dr. Arcan F. Dericioğlu
Ortak Tez Yöneticisi: Prof. Dr. A. Şakir BOR

Kasım 2014, 105 sayfa

Fiber metal katmanlı kompozit malzemeler, hava araçlarının yorulmaya hassas bölgelerinde kullanılmak üzere son 20-30 yılda geliştirilen yeni malzemelerdir. Bu lamine kompozitler yüzeyi uygun hale getirilmiş metallerle fiber takviyeli polimer matrisli kompozitlerden meydana gelirler.

Bu malzemelerin üretiminde metallerin yüzey hazırlık işlemleri önem arz etmekte ve farklı disiplinlere ait yüzey mühendislik bilgilerini gerekli kılmaktadır. Kullanılan metallerin yüzeyleri kirlilikten ve nemden arındırılmış olmalı ve istenilen mekanik dayancın sağlanabilmesi için nihai kompozit malzemede mevcut hava boşluğu miktarı olabildiği kadar düşük olmalıdır. Dolayısı ile sıvının/reçinenin ıslatma kabiliyeti yüksek, katı/metal yüzeyinin ıslanma kabiliyetinin uygun hale getirilmesi gerekmektedir. Kimyasal aşındırma, anodize etme, plazma püskürtme, lazerli doku oluşturma, silan ve/veya sol-jel vb. yöntemleri birlikte veya ayrı ayrı olarak endüstride yüzey hazırlama işlemleri olarak uygulanmaktadır. Fiber-metal katmanlı kompozitler kimyasal aşındırma-anodize etme ve yapıştırıcı ile prepregi otoklavlama gibi uzun-

yorucu-pahalı olmalarının yanında çevreye de zararlı üretim yöntemleri ile üretilmiş ve araştırmalar buna göre yapılmıştır.

Bu tez çalışmasında, 2024 T3 aluminyum alaşımının yüzeyinin hazırlığı zımparalama ve γ-glycidoxytrimethoxy silan uygulamaları ile, fiber-metal kompozit üretimi ise vakum infüzyon tekniği ile yapılmıştır. Gerilim-gerinim, yük-yer değiştirme ilişkileri ve kompozitin her iki taraftaki arayüz özellikleri uygulanan yüzey hazırlık işlemleri ile kontrol edilen yüzey pürüzlülüğü-temas açısı ve yayılma kabiliyetine bağlı olarak incelenmiştir. Elde edilen sonuçlar, vakum infüzyon tekniğinin fiber metal katmanlı kompozit malzemelerin üretimi için başarılı bir alternatif olduğunu ortaya koymuştur.

Anahtar Sözcükler: Fiber metal katmanlı kompozitler, vakum infüzyon, silan, 2024 T3 aluminyum alaşımı, yüzey ön hazırlığı, pürüzlülük, temas açısı, yayılma.

For my son Kemal Demir and my wife Sena;
to my precious mom Mefharet and dad Cengiz,
my mother and father in law Nilüfer and Aydın,
my Fu-Ahu Meryem and Zo-Umut,
my brother in law Mehmet.

ACKNOWLEDGEMENTS

I am very grateful to my supervisor Assoc. Prof. Dr. Arcan F. Dericioğlu for his friendship, guidance and support during this work, and his great attention and patience on me from the beginning until the end of my graduation.

It is great pleasure to thank my co-supervisor Prof. Dr. Şakir Bor, Prof. Dr. Cevdet Kaynak for his always smiling face, Prof. Dr. Ali Kalkanlı for the strength he gave me all the time, Prof. Dr. Rıza Gürbüz and Prof. Dr. Bilgehan ÖGEL for joyful sailing synergy.

I am very grateful to my laboratory colleagues Simge Tülbez, Sıla Atabay, Mert Güney Bilgin, Özgür Hamat, Erkan Aşık, Bensu Tunca and especially to Aylin Güneş and Assist. Prof. Dr. Halil İbrahim Yavuz for their support and friendship at every stage of this work and my graduation.

I am very grateful to METU Metallurgical and Materials Engineering Department for all the support provided during this study. I want to thank to Assist. Prof. Dr. Orhan Akar/METU MEMS for his cooperation and help for optical profilometry study.

I want to thank to my family, for their great patience, not only during this work but also at every stage of my life.

TABLE OF CONTENTS

LIST OF TABLES

TABLES

LIST OF FIGURES

FIGURES

CHAPTER 1

INTRODUCTION

Modern aircraft design needs to investigate and reveal the fatigue cracks before they reach the critical crack length so the structural materials must provide this tolerance like fiber metal laminates (fail safe design criteria) [1]. A permanent interest during the last decades with newly emerging questions about fatigue resistant, high strength and stiff materials have been satisfied by fiber metal laminates with their unique and favorable properties [2]. Fiber metal laminates are improved hybrid composites, combining strong fibers with ductile aluminum layers, and show outstanding properties with their being light weight [3].

Fiber metal laminates are the most emerging materials to be used as composites in aviation industry because of their excellent fatigue and impact resistance, machinability and formability properties along with their suitability for inspection after impact [4]. Fiber metal laminates combine the best properties of the matrix and the fiber where they do not include the individual disadvantages of the two constituents [1]. Fiber metal laminates have an important advantage over the conventional composites being resistant to UV and moisture absorption, where they are superior compared to monolithic aluminum in terms of their sensitivity to fatigue cracks. Additionally, besides fabrication, quality control, plastic deformation, characterization

and time dependent tests, cutting is another prominent issue about the handling of the fiber metal laminates [5].

Crack bridging mechanism of fiber metal laminates makes them superior damage tolerant composites, while they show monolithic metal and composite behavior at the same time [6]. Towards building safer aircrafts, fiber metal laminates have some excellent features such as yielding, energy absorption and electrical conductivity against monolithic aluminum or fiber reinforced composites [7]. Furthermore, hybrid composite materials which consist of metals and fiber reinforced composites have very good electromagnetic shielding properties besides their superior mechanical aspects [8]. With their low costs and improved safety, fiber metal laminates offer very important benefits with their lightweight and damage tolerant characteristics which combine durability along with fatigue, corrosion and impact resistance [9].

Moreover, fiber metal laminates have excellent residual strength and flame penetration resistance [10]. Comparing with monolithic aluminum, fiber metal laminates show excellent crack propagation shielding because of their unique structure. Although they have been designed for fatigue prone areas, fiber metal laminates combine various advantageous properties in one single material with a low cost solution [9]. Their lower density, crack bridging capability and adaptability to specific demands of the designer make them considerably advantageous compare to monolithic aluminum and fiber reinforced polymer matrix composites [5].

Properties of the fiber metal laminates can be tuned according to the load. Fiber metal laminates provide capability for the detection of cracks, dents, scratches and lightning strike damages just like monolithic metals [6]. A dynamic impact damage may cause catastrophic failure to the monolithic aluminum or fiber reinforced composite alone whereas fiber metal laminates respond to the dynamic impact like a monolithic metal yet preventing the damage to develop because of the crack bridging provided by the fibers transforming the energy into inelastic deformation [7]. With all of the above mentioned advantages of the fiber metal laminates, the design criteria allow the

designers to accept fiber metal laminates as monolithic aluminum without the need for some additional reinforcements [1].

Prepregs together with degreased-etched-anodized aluminum have been widely used in aviation industry to fabricate fiber metal laminates utilizing high pressurized autoclave for bonding [10]. The autoclave manufacturing process is a long batch, and expensive process restricting its own potential for automation [11]. Autoclave-prepreg system creates residual stress in the final component whose magnitude changes according to the thickness of the material. Residual compressive stress in the fibers, and tensile stress on the aluminum alloy render post stretching necessary resulting in additional costs [1].

It is very hard to fabricate fine quality fiber metal laminated composite because the manufacturing process is very complicated and difficult to control. Metal-prepreg, prepreg-prepreg interfaces contain porosity which results in the inferior mechanical properties of the final product because of poor adhesion [12]. The prepreg materials used with autoclave processes have high stiffness, as a result they cannot be shaped in complex geometries. Because of these drawbacks automotive industry still cannot use these materials under automation except for custom fabrications [11].

Vacuum infusion is a popular composite manufacturing technique. Compared to prepreg-autoclave manufacturing, the consumables used in vacuum infusion have higher shelf life, and there will be no need for large ovens, heat and pressure [11]. In industry vacuum infusion process has been used to handle large composite parts with low costs making it the most popular in different industries like aviation, transportation, marine and power units production. It is a composite manufacturing technique requiring a low viscosity resin to wet a dry preform (fibers) under negative pressure gradient [13]. Another important property of vacuum infusion is its applicability to complex shaped products. Composited fabricated by vacuum infusion show better mechanical characteristics, consistency and repeatability than the ones fabricated by hand lay-up or spraying techniques [13]. In the near future, it is expected

that the industry will pay special attention to vacuum infusion, because it is feasible against prepreg-autoclave process while it is also providing superior mechanical performance compared to hand lay-up [11].

Joining is a key processing step in going from parts to components. Because riveting or longitudinal lap joints create high stress concentration areas, adhesive bonding is accepted to be a very efficient technique for joining aluminum structures [14]. Widespread scientific activities are ongoing about preparing surfaces properly for adhesive bonding. Chromic acid anodizing process has widely been used on surface pretreatment yet it has very important disadvantages as a result of which aerospace, automotive and defense sectors are paying attention to replace it.

For long term service life of vehicles, good surface preparation carries importance for adhesive bonding process. Surface pretreatment technologies being used for aluminum alloys are not environmental friendly. There are some chemical etching processes like chromic-sulfuric acid, Forest Product Laboratory (FPL) and sulpho-ferric acid etching processes which are intermediate steps before anodizing processes. DC and AC anodizing processes follow these etching processes to create passive porous oxide layer, which are hazardous because they contain strong acids and hexavalent chromium. Beside these hazardous chemicals, there are alternative surface pretreatments involving environmental friendly coupling agents like silane and sol-gel which must be developed for their applicability in industry [15].

The fiber-resin interfacial integrity provides the mechanical strength to the composite structures [16]. Insufficient adhesion because of porosity and void content leads to stress concentration which creates delamination or cracks which have detrimental effect on mechanical strength. Interface is the most important and central point to be understood under interdisciplinary approach which creates a successful composite with acceptable mechanical strength [12]. Increasing the bonding strength of the interface between the metal and the fiber reinforced composite plays an important role on the durability of the final fiber metal laminate product [8].

Consequently, during the adhesive joining of aluminum structures special attention has to be paid to the interfacial integrity and compatibility. In this scope, there must be some primers to be used with Grid blast silane (GBS) treatment. A practical surface pretreatment system must be developed for fiber metal laminates because the interface determines the durability of the final composite. The main aim of intermediate degreasing-anodizing-post treatment steps are to handle an uncontaminated and roughened surface with stable oxide layer to increase the surface adhesion area [10].

Wetting optimization is the most important issue for the surface preparation. Practical processes in the industries like aviation, automotive, high speed trains, armored vehicles, naval architecture require spreading of a liquid on a solid which is affected by the interfacial phenomena including thermodynamic wettability at equilibrium state, contamination, hysteresis of the contact angle of the liquid on the solid, roughness of the solid and spreading of the liquid over the solid [17]. Interfacial tensions of liquid and solid plays an important role on the wetting with capillary origami and roughness where pressure gradients over them drive the fluid flow [18].

Good wettability of a substrate surface by a liquid or adhesive is vital for a sufficient bond which constitutes the properties of both sides including surface wettability, surface energy and spreading phenomena according to roughened topography [19]. Critical issues of wetting belonging directly to the nature of the solid and liquid surface forces, dramatically change the bonding strength with their behavior to characterize the bonding area chemically, thermodynamically or geometrically which include contact angle-roughness relationship [20].

Fiber metal laminated composites have been fabricated with prepreg-autoclave processes to combine the metal and the adhesive with fiber reinforced polymer matrix composites until now. In addition to this, some experimental efforts have been experienced about fabricating such materials using VARTM process. This study aims to fabricate fiber metal laminated composites by vacuum infusion process and to optimize the aluminum surface topography to reach to the mechanical characteristics achieved in these materials by prepreg-autoclave processes. Vacuum infusion is

considered to be an alternative method for the fabrication of the fiber metal laminates being low cost-easy labored process rather than the long-batch and expensive processes of “etch-anodize-adhesive primer-prepreg-autoclave” including process cycles.

CHAPTER 2

LITERATURE REVIEW

2.1. Fiber Reinforced Plastics

This definition is also referred as fiber reinforced polymer matrix composites which is made of reinforcing materials as fibers, chips etc. and polymeric materials to surrender the fiber dozens hold together and transferring the load to them [11]. Thermoplastics and thermosets are being widely used to as matrix materials. And as reinforcement materials aramids, glass fibers, carbon fibers are being widely used which boron fibers, metallic fibers etc. are beneath them.

2.1.1. Glass Fibers

Glass fibers can be classified as;

a) E-glass (improved electrical resistance)
b) S-glass (high strength)
c) C-glass (high chemical resistance).

2.1.2. Carbon Fibers

Carbon Fibers can be classified as;

a) Polyacrylonitrile (PAN) fibers,

b) Pitch or,
c) Rayon fibers through production processes.

Through heating, raw material loses most non-carbon atoms in the chain and processing also aligns carbon chains with very high modulus (stiffness).

2.1.3. Aramid Fibers

Aramid fibers have the greatest strength and modulus properties of organic fibers and Kevlar is the most commonly used aramid fiber. Aramids are strong and stiff but their greatest value is in impact applications like;

a. Front side of airplane wings,
b. Armor applications.

After manufacturing the fiber they can be found from the market in the different forms like; packages on spools called tows, chopped fibers (including whiskers), mat (random),woven fibers, tapes and manufactured as prepreg.

Although they've got lower mechanical properties, the cost of glass fiber reinforced composites create interest to build big-large components against carbon reinforced composites to use under non-extreme weather conditions [21].

When we use the term composites during daily life, generally it's understood that we're intending to talk about fiber reinforced-polymer matrix composites. We prefer "daily life" saying because composite materials occupied lots of materials' place in the recent decades and become mostly used preferential because of their specialties like; strength with low weight – low cost for most applications except aerospace industries etc., long term service capability, long term durability, their excellent fatigue strength, damage tolerance, impact absorbance etc [11].

2.2. Fiber Reinforced Polymer Matrix Composites

Manufacturing processes and used materials to manufacture composites differentiate. If it's tended to classify the materials that being used in fiber reinforced polymer matrix composites and manufacturing from a general scope the details below can be specified.

2.2.1. Resins:

Thermoplastic resins which are generally used with short fibers, while thermoset resins those can be used with long fibers, which are preferential because of strength but got an issue about being environmentally friend consumable that must be developed because of recycling problems [13].

Resin as matrix decides the outer performance of the composites against thermal resistance, fire resistance, proper surface condition and photooxidation resistance [11].

2.2.2. Fibers:

Short fibers which are less than 0.2 inches (whiskers), which are being processed through standard thermoplastic processes, while the final product must pass through gates, runners, and gaps between processing screw and barrel walls. Intermediate length fiber reinforcements which are longer than whiskers, carry difficulties to coat them enough to reap strength benefits, low viscosity thermosets to "wet-out" the materials better than high viscosity thermoplastics and generally used with unsaturated polyester and vinyl ester resins. Continuous fibers, which are well known as very long fibers, are being typically used with thermosets, used generally in advanced composite parts and have greater material property requirements. If we tend to classify the manufacturing methods;

- Thermoplastic processes –Very short fibers
- Matched die/compression molding

- RTM
- Spray-up
- Hand lay-up for wet and prepreg materials
- Filament winding and fiber placement
- Pultrusion
- VARTM-Vacuum Assisted Resin Transfer Moulding
- VAP-Vacuum Assisted Processing.

2.3. Composite Manufacturing Processes

Brief explanations will be given here about the most important composite manufacturing processes.

2.3.1. Hand Lay-Up

Hand (wet) lay-up consists of placing the preform on the mold and then applying resin by brush or roller or spray. This is the cheapest way of any composite manufacturing method [11].

In the marine industry, where enormous parts are being produced hand lay-up process is the most widely used fabricating technique [22].

Only one smooth surface is achieved, controlling the volume fraction of the fiber and the resin and the thickness according to these is severely limited. Typical advantages of hand lay-up processes are low cost tools and versatile: wide range of products. And the disadvantages are time consuming, unhealthy situation for the labor because of the hazardous gases that resins release, easy to form air bubbles and disorientation of fibers which can create inconsistency and decrease the mechanical strength severely.

2.3.2 Prepreg Forming

No other composites processing method has yielded the properties and repeatability as high as autoclaving of prepreg materials [11].
For most aerospace applications, prepreg is the preferential method because of its' high mechanical strength according to low void content and optimum resin volume.

Pre-impregnated is the source of the word "Prepreg". During prepreg's manufacturing process, the resin is being separated to the fabric with high pressure and partially cured to keep its bonded situation.

A manufacturer who is using prepreg must put it on a mold (Figure 2.2) and complete the curing under the temperature and pressure needed. There are autoclave oven assemblies with high pressure and heat to step up to the curing and finishing parts and the process can be made automated if preferred [23].
The autoclaves are very important devices to handle the best mechanical properties with optimum volume fractions of fiber and the resin. Because of the impregnation phenomena during the production step of prepreg itself, void content between fiber and the resin decreases under 2% which makes the prepreg forming preferential for aerospace industry with its high strength/weight ratio [24].

Although its excellent properties, prepreg has got some disadvantages like high cost, short shelf life, supplying conditions that necessitate controllable temperature and moisture conditions [11].
Also it's not so easy to fabricate complex shapes with prepreg because of its' being partially cured-which makes the material stiff. The manufacturer who uses prepreg must concern after every sheet lay up to pressurize the mold and control implementing void, delamination or not.

Fabricating the GLARE® with prepreg in autoclave makes the production step very expensive and has got constraint in dimensions [25].

2.3.3. Vacuum Bagging

Vacuum bag molding, a refinement of hand lay-up, uses a vacuum to eliminate entrapped air to decrease the void content and excess resin. Until the resin cured the vacuum bag keeps the mold insulated from air. The pressure difference between the mold and the atmospheric pressure outside of the mold, a kind of clamping would be forced to the composite inside so better and sophisticated parts can be manufactured. Vacuum bagging has got a simple design with any fiber/matrix combination which has better quality for the cost. At the same time, it depends to the labor to handle the consistency desired. During vacuum bagging, heating up is limited so moisture can captured to the mold and can be slow [26].

2.3.4. Filament Winding

Filament winding consists of winding continuous roving of fiber onto a rotating male mandrel in predetermined patterns to product compressed air tanks, sail boat masts, light poles, high pressure tanks of CO2 etc [27].With this process, many different fibers and resins can be used to achieve desired characteristics for the finished component. This method of manufacturing composites provides good control over fiber placement through uniformity of the structure but optimizations are still being developed numerically [28].Parts with huge sizes can be fabricated by filament winding process but shape of the product and heat treatment after fiber placement can push the manufacturer to spend afford and additional money.

2.4. Fiber Metal Laminates

Fiber metal laminates are composites that are brought together to get the best properties of each metal and fibers which united with a resin. Fiber metal laminates combine the best properties of each material that consist them [28].

Fiber metal laminates with their low weight, they’ve got very good fatigue, impact properties with fire and corrosion resistance [30]. Fiber metal laminates carry the

outmost properties of the material that are being composed which are thin metal sheets and the composites [25]. Multiple metal plies that are laminated with adhesives increases the fracture toughness of monolithic aluminum with the same thickness [31]. Fatigue behavior and crack impeding properties in fiber metal laminates are better than monolithic aluminum [32]. Damage tolerance of laminated titanium is better than monolithic titanium at the same thickness [33].

GLARE® is glass fiber reinforced laminate for advanced aircraft structures which carries the properties like outstanding fatigue resistance, flame retardance with burn through resistance, excellent impact resistivity, residual strength, blunt notch resistivity, good corrosion resistance, good damping, insulation and easy repairment availability[30].

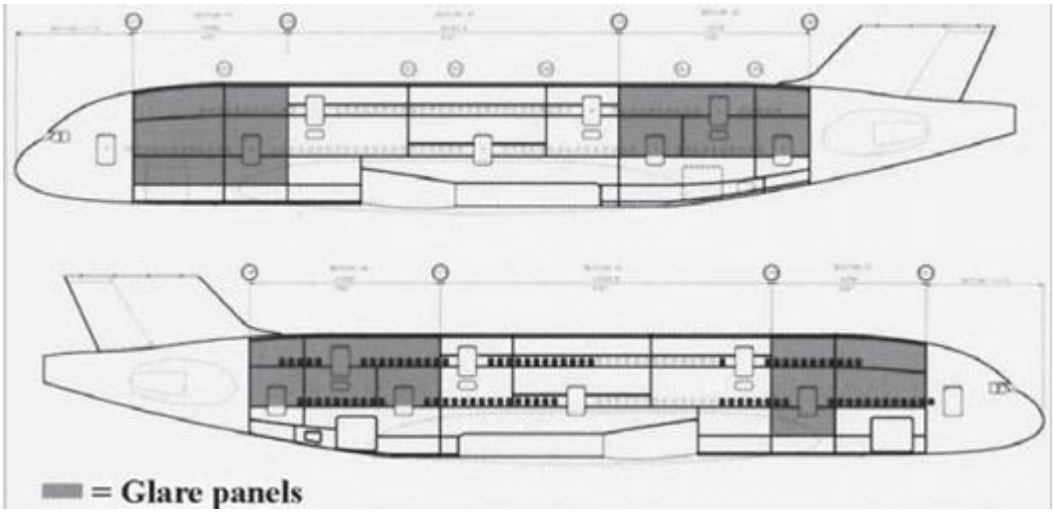

Figure 2.1. Glare® areas in Airbus A-380.0.1[30].

Between others lower density, crack bridging of the fibers –which creates excellent fatigue resistance-, tailoring against mechanic demands by orientation of the fibers can be told mechanically advantageous compared to monolithic aluminum [5]. Fiber metal

laminates give capability to inspection just like metals which decrease the costs because of increasing the inspection periods [29].

In the last three decades fiber metal laminates are the emerging new fuselage and wing materials because of their excellent fatigue (shown in fig.1), damage tolerant, impact resistant and flame retardant properties with low inspection intervals, repairment feasibility -with different techniques which increases damage tolerant nature and blunt notch strength of these materials over monolithic 2024 T3 aluminum layers according to complex failure modes [9].

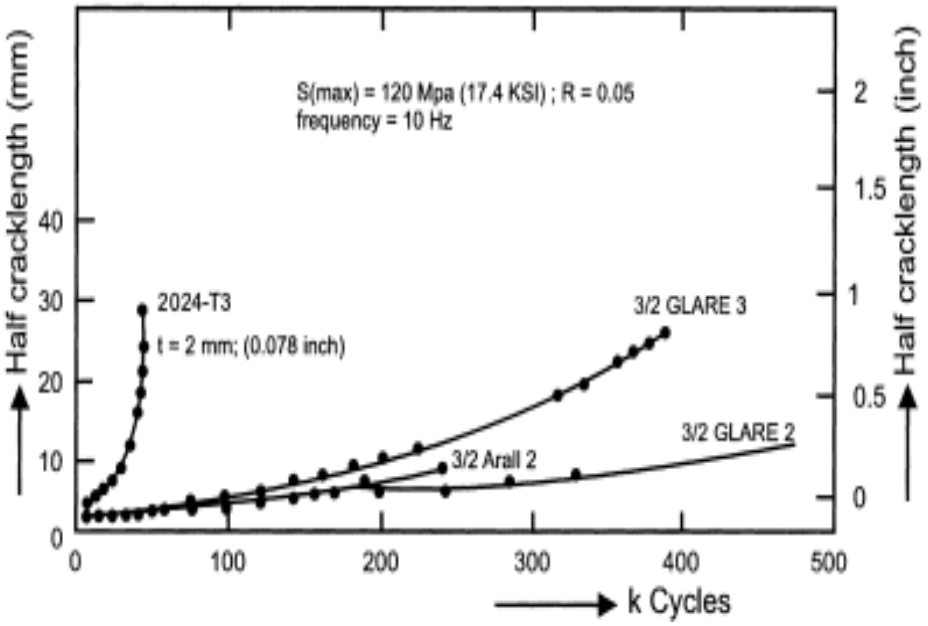

Figure 2.2. The crack growth behavior of unidirectional Glare® 2, Cross plied Glare® 3, Arall® 2 and 2024 T3 for a fuselage loading [30].0.2

Fiber metal laminates show good durability against thermal fluctuations and are stable in cryogenic environments. There have been investigated fiber metal laminates for decades to use in the aerospace industry with different kinds and with different materials like ARALL®, CARALL® and GLARE®.

ARALL® carries the meaning aramid reinforced aluminum laminate, which tried to be specified from 1980s to use in the wings of the airplanes.

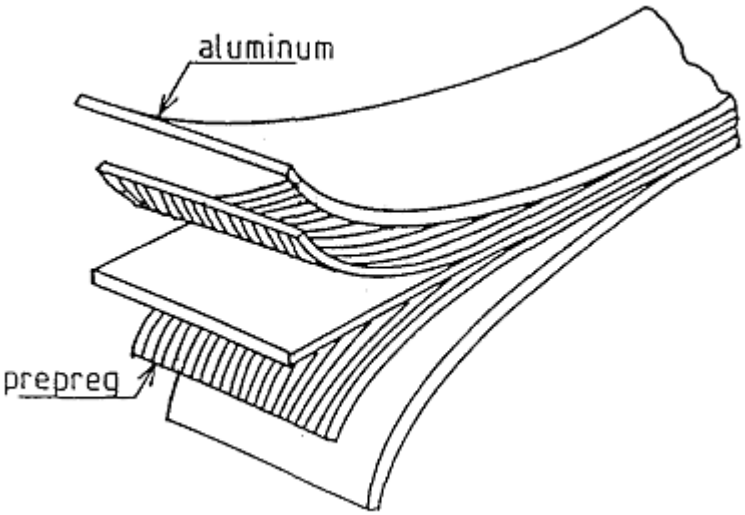

Figure 2.3. Schematic ARALL® arrangement[34]..0.3

ARALL® is the first metal laminate and it's discovered and seen later that under compressive loads aramid fibers response very bad [34].

CARALL® that has the meaning carbon fiber reinforced aluminum laminate developed and at the beginning of the 1990s, GLARE® which means glass fiber reinforced aluminum laminate has been developed to use in the airplanes for civil transportation.

GLARE® can be compared to aluminum monolithic sheet and if the advantages must be said it must start with the low density with excellent fatigue behavior according to fiber bridging of the fiber and the materials' giving ability to be tailored fort the design values of the strength in the area that wanted to be carried by the orientation and the arrangement of the fiber [5]. Because of better compressive behavior of glass, GLARE® has been developed in 1991 [35].

Aramid is the fiber which has got the highest strength in composites but at the same time has got an disadvantage that is very important for a flying vehicle: it's heavy. After trials in some special parts like doors etc. lighter but similar load carrying carbon fibers are tried for the applications. But carbon with its all strength has poor ductility. Because of its high stiffness shaping and tailoring the CARALL® is not so easy.

From the fatigue point of view GLARE® gives an advantage with its fiber bridging capability when a crack starts to propagate and because of its load transferability it increases the design stress values while it decrease the crack propagation speed. (fig.2.9)When a fatigue crack nucleates and starts to propagate fibers are partly banning and slowing the propagation but these phenomena promotes a shear load between fiber and the aluminum sheet. According to this shear load occurrence, thinning the aluminum sheet while increasing the number of the aluminum sheets to handle the same fiber metal laminate thickness, small fatigue cracks will be carried and banned by the GLARE® with its separating the shear loads to concentrate at smaller parts-smaller delamination [5].

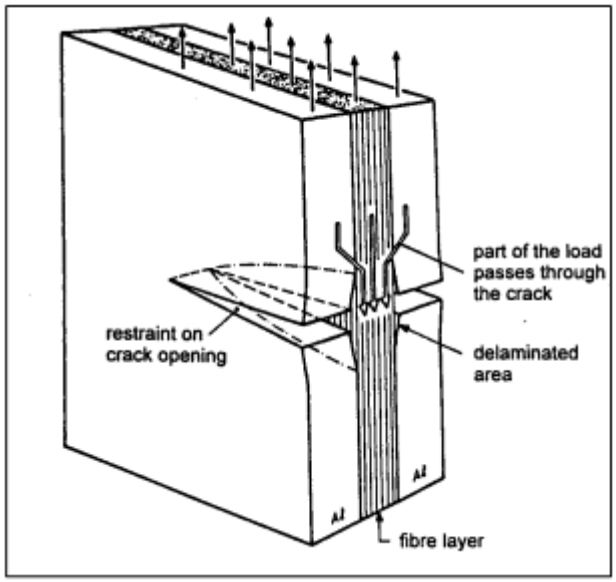

Figure 2.4. CRACK bridging [5].0.4

For monolithic aluminum, it is very easy to inspect and consider the damage because its being visible on the sheet therefore the damage size can be recorded and the remaining life of the material with the residual strength may be calculated analytically.

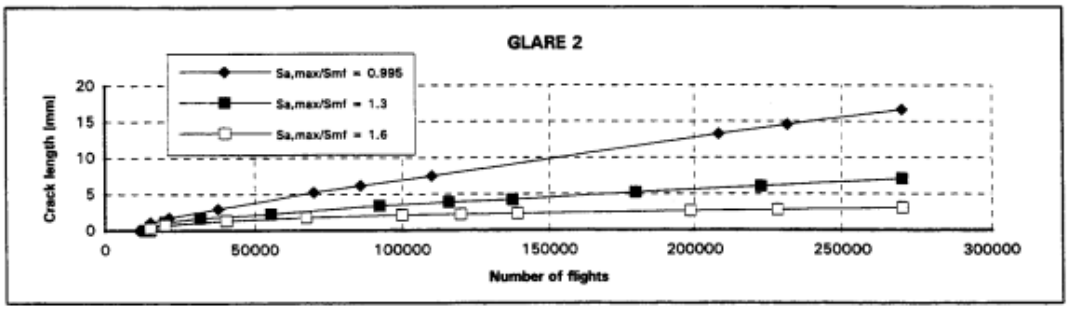

Figure 2.5. Fatigue life of Glare® [5, 36] 0.5

The impact damage detection and the chase of the damage is the same for GLARE® with the monolithic aluminum but GLARE® has a real advantage because of fiber crack bridging which bans/slows the propagation and carries significant loads. But in an unexpected-not followed-incident situation R-curve approach can be approximated to the GLARE® just like monolithic aluminum [6].

From the machining and bending point of view, the GLARE® is being accepted as a metal in the literature and the acceptance criteria of the airworthiness directives. To machine and to bend the glare® is possible -which is not for normal composites-so glare® can be accepted as a metallic structure [5].

2.5. Surface Pretreatments

Surface treatments must be tailored excellent to get the long term service life for adhesive bonding applications for the aerospace industry [15].

Low joint strength, failure modes of fracture, delamination during adhesion or after loading emerge up to decreased strength of adhesion. Before the surface treatment some issues must be under control to get the best result of adhesion like; contamination free area, mechanical stability, roughness optimization, wettability with the chemical used during the process and hydrolytically stability [37].

Additionally, void content of interface in the adhesion zone, authorize the strength of adhesion, which creates a crack nucleation point except contamination creates a stress concentration. Proper roughness must be attended to increase the surface area of adhesion. Moisture and thermal exposure creates hydrothermal aging which promotes failure of adhesion by nucleation of fracture at the entanglement of small delaminations under mixed modes of loads during exposure [38].. Hydrolytically stabilized interface will be dominant for long service time against delamination of moisture failure. The most important issue to understand the failure mechanisms of adhesion is the interface zone between organic and the inorganic materials as shown in Fig. 1 [15]

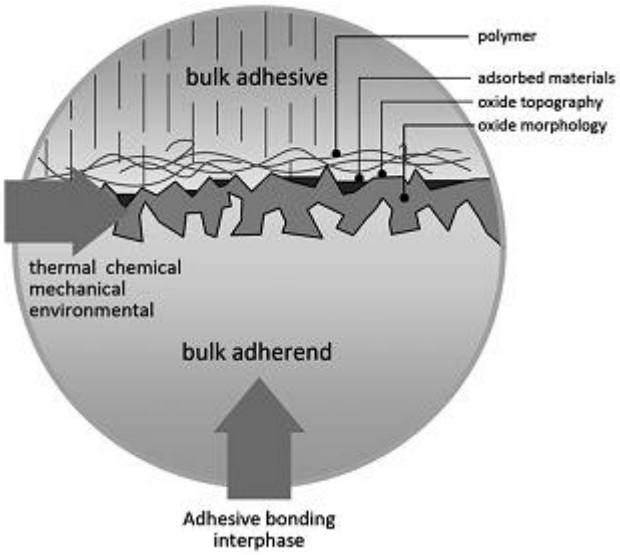

Figure. 2.6. Adhesive Bonding Interface [15].Figure 6

0.7

There are several surface treatments to modify, optimize and/or prepare the aluminum surface for proper adhesion, which are summarized in Table 2.1.

Table 1

Table 2.1. Summary of Surface Treatments on Aluminum Alloys [15].

Treatments	Nature of treatments	Reference sources
Grit-blast with alumina particle	Mechanical	19,21–42,46
Cryoblasting	Mechanical	28
Forest product laboratory (FPL) – including chromic acid etching	Acid etching	21–23,25,26,28,31–33,39,41,43–47,49,51
Sulfo–ferric etching (P2)	Acid etching	44,48
Phosphoric acid anodizing (PAA)	DC-anodizing	19,22–24,26,28,31–34,38,39,43,44,46–55,64
Chromic acid anodizing (CAA)	DC-anodizing	19,21,24,36,54,56,57
Phosphoric-sulphuric acid anodizing (PSA)	DC-anodizing	57,58
Boric–sulphuric acid anodizing (BSAA)	DC-anodizing	21,54,59,60
Sulphuric Acid Anodizing (SAA)	DC-anodizing	47,48,51
AC phosphoric acid anodizing (AC-PAA)	AC-anodizing	18,43,51
AC sulfuric acid anodizing (AC-SAA)	AC-anodizing	18,43,45,47,51
Silane	Coupling/oxidation	22,24,25,29,30,31,35–37,39,40,50,52,61–65
Sol-gel	Coupling/oxidation	34,38,41,42,46,48
Excimer UV laser (Laser)	Mechanical	30,34,35,66–69
Plasma-sprayed coating (Plasma)	Ablation/oxidation	32,36,56,70–73
Ion beam enhanced deposition (IBED)	Ablation/oxidation	33

Aerospace industry prefer to use the anodizing methods, which has been used for nearly fifty years, just because it gives dependability with it's been experienced widely. However, all R&D activities about the hybrid composites/metal-organic compound material researches around the world, struggles to find out to not to use the chemicals that are hazardous and does not response for recycling which contain hexavalent chromium, strong acids etc. with chromic acid anodizing, phosphoric acid anodizing etc. A brief knowledge will be given about several surface treatments in this chapter.

2.5.1. Electrochemical Surface Treatments

Chromic Acid Anodizing and Phosphoric Acid Anodizing are widely used electrochemical processes in different unions and districts of aerospace industry. Experiments showed that these anodizing types were preferred to bond the metallic parts, but hazardous materials like strong acid and hexavalent chromium are being used during these processes [15].

Limitations of hazardous chemicals of these methods is the driving force for attending to find out other proper solutions with the same strength, durability and porosity needed.

2.5.2. Chromic Acid Anodizing-CAA

In this type of anodic process, first current with the same level of at 40 volts DC followed by a second level at 50 volts DC as would be enough [39]. CAA process which has been used in European aerospace industry creates thicker and more amorphous surface layer than phosphoric acid anodizing.

2.5.3. Phosphoric Acid Anodizing-PAA

PAA is currently the preferred anodizing option for primary bonded structures in the United States. The PAA-processed area of the sample gives possibility to good capillary forces on the chemical and/or adhesive, so there will be strong enough interlocking to create a good adhesion [40]. PAA gives better durability than CAA but static strength of lap shear tests are similar.

2.5.4. Phosphoric-Sulphuric Acid Anodizing –PSAA

The PSAA process was developed by DaimlerChrysler Aerospace Airbus which does not include hazardous chemicals like chromic acids. The process is simple it is giving the industry motivation to use with its reliability [41].

2.5.5. Sulphuric Acid Anodizing

Sulphuric Acid Anodizing gives really good results for protective coating and painting, and giving an opportunity to create wide scale of oxide thicknesses on aluminum alloys [15]

2.5.6. AC Anodizing

SINTEF Materials Technology and Norwegian University of Science and Technology develops AC anodizing process which is different on the main practice from the other anodizing processes [42].

This alternative is a highly feasible, robust, and environmentally friendly process, which is free from the hexavalent chromium found in the conventional CAA. The main differentiation of AC anodizing from DC anodizing is hydrogen gas is being produced by the surface of the sample which eliminates the contamination near anodizing.

2.5.7. Coupling Agents

During the last decades environmental friendly coupling agents are being optimised to use like silane, sol-gel etc.

2.5.7.1. Silane

Silane is going to be explained in detail with its application method later in this thesis. But to give a brief information about silane the thickness and the chemical bonding type of it must be emphasized near its environmental friendly structure.

Aqueous γ-glycidoxypropyltrimethoxy silane (γ-GPS) solution has got between 1.5-2.9 nm. This coupling agent is making the bond between the oxide of the metal substrate and the organic compound of the resin with its propyl chain. Thousands of

adhesively bonded repairs using silane techniques have been applied to military aircrafts over the past 25 years [15].

Rider and Arnott [43]. gave descriptions about the silane treated surface are being hydrolytically stable and strengthens the bonding interface, increases the durability. Abel et al. [44]., showed whit time of flight secondary ion mass spectrometry, well bonded Al-O-Si couple experienced between silane solution of γ-GPS and aluminum substrate. The crack growth was propagated through the interface (‘‘composite-zone’’) between oxide, silane, and adhesive in cohesive failure mode, which is considered as an optimum type of failure that occurs primarily in the adhesive layer [15].

2.5.7.2. Sol-Gel

Another option, i.e., sol-gel, a contraction for solution- gelation, which involves the growth of metal-oxo polymers through both hydrolysis and a condensation reaction to form inorganic polymer networks in thicknesses ranging from 50 to 200nm.

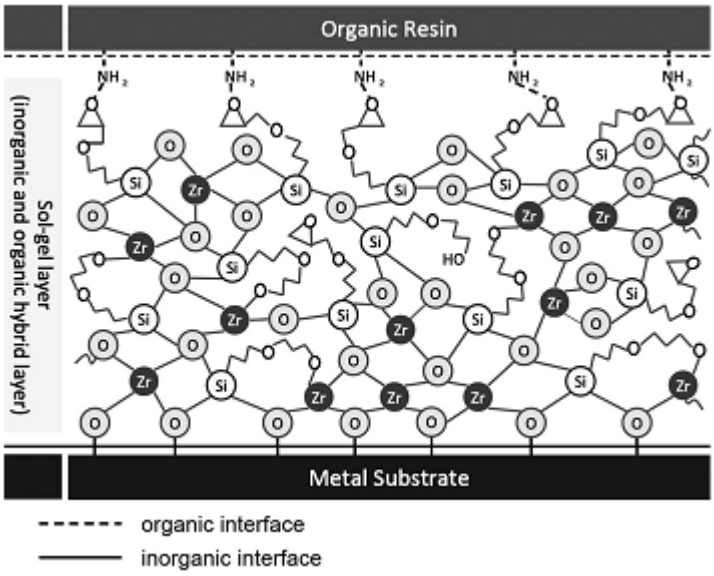

Figure 2.7. Typical sol-gel thin film representation [15]. 0.1

Instead of these conventional wet chemical processes, dry surface treatments like excimer laser texturing, plasma sprayed coating and/or ion beam enhanced film deposition techniques can be used. E of hazardous chemical processes but they must be optimized for the strength and the durability with the cost feasibility.

2.5.8. Mechanical Surface Treatments of Aluminum

Mechanical abrasion is the preliminary step for cleaning the hazardous oxide layer and to get a optimized rough surface [15].

It is being achieved by abrasion with sand paper, special pads by hand/machines or stood for alumina grids with sand blasting. Mechanical surface treatments create a surface activation which establishes macro roughness before other surface treatments like silane, sol-gel, plasma oxidation etc.

2.5.9. Chemical Etching of Aluminum Surface

Chemical treatment is an intermediate preparation between removing the contamination, cleaning with some chemicals like MEK, toluene etc., and electro-chemical process. Chemical etching should be in accordance with the fore-treatments, i.e., an anodizing process [15].

Different companies in different countries prefer different methods of chemical treatments like FPL-Forest Product Laboratory dichromate sulphuric etching, CAE-Chromic Acid etching and sulpho pherric etch.

Some airworthiness directives and/or journals have been declared that adhesive bonding after FPL method has got serious issues to solve about durable bonding. After all, the FPL process that dichromate-sulphuric acid is being used during it, still is a common and widely used process to handle chemical etching with 40 nm passivized oxide layer by the aerospace industry [37].

To replace FPL that uses very hazardous chemical-sulphuric dichromate- sulpho-pherric chemical treatment is being used which has been called P2 process too [45]. P2 creates thinner oxide layer than FPL, which is like 37 nm.

These chemical treatments which modify the surface of the substrate are not suitable to use as stand-alone but intermediate step before anodizing.

2.6. Fracture Analysis

GLARE® is glass fiber reinforced laminate for advanced aircraft structures which carries the properties like outstanding fatigue resistance, flame retardance with burn through resistance, excellent impact resistivity, residual strength, blunt notch resistivity, good corrosion resistance, good damping, insulation and easy repairment availability.

Fiber metal laminates shows excellent properties of both metal sheets and fibers while impeding or catching crack with perfect damage tolerant and impact resistant structures of them even though they got low density. Through thickness corrosion resistance response is much better than monolithic aluminum. Aluminum layer prevents the material from UV and moisture, if the moisture goes in from the first layer/outer layer of the aluminum-first layer of glass fiber capture it so prevents the rest of the fiber metal laminate from moisture [46].

The tensile properties of unidirectional GLARE® shows better results and transverse GLARE® shows lower results from longitudinal monolithic aluminum.

High strength glass fibers give to the glare® higher tensile strength, compressive strength and adhesive ability relative to aramid fibers because glass fiber offers good cross-ply orientation. Volume fraction of the orientation of fiber determines the tensile and flexural strength of glare® laminates and for tensile loads 45 degrees stitched mat and for flexural strength woven roving had greater properties.(fig.2.14)

Table 2.2. Tensile properties of 3 different orientation of fibers [46]. Table 2

Orientation	Maximum breaking load (N)	Ultimate tensile strength (N/mm^2)	Displacement (mm)	Thickness (mm)
CSM	8150	95.68	8.24	3.10
Woven roving	11631	150.08	9.69	3.48
45^0 stitched mat	32495	307.28	11.15	4.50

Table 2.3. Flexure properties of 3 different orientation [46].**Table 3.**

Orientation	Maximum breaking load (N)	Ultimate bending strength (N/mm^2)	Displacement (mm)	Thickness (mm)
CSM	167.13	320.719	5.75	3.10
Woven roving	310.60	308.62	3.90	3.48
45^0 stitched mat	223.33	208	3.86	4.50

If we choose to use glass fiber with low modulus, the elastic moduli of the GLARE® decreases. It is not sufficient to predict the mechanical response of fiber metal laminates simply because of the elasto-plastic behavior of the aluminum and the residual stresses after curing. There must an analytical systematic to be developed to make predictions about the inelastic behavior of GLARE® after the yielding of aluminum layers [47]. During tensile test in the longitudinal way, fiber pull-outs, interface – matrix shear have been seen in composites [48].

Elastic modulus in tensile and compressive properties of GLARE® laminates, are nearly same because of tensile and compressive behaviors of fibers. All of the layers of the glass reinforced aluminum laminates face the same deformations under tensile loading. The mechanical response of composite in fiber metal laminates must be

accepted linearly elastic. Because of aluminum shows plastic response for a very long time after yield point, total fiber metal laminate shows nonlinear tensile behavior and an approximation that accepts normal stress-strain relation does not give adequate results [30].

If the notch size gets bigger, the blunt notch resistance increases in GLARE® due to the static delamination of fiber reinforced composite which levels off the stress and delay fiber fracture in/near the hole.

The compressive yield strength of GLARE® is lower than tensile yield strength but because of their good response to compressive loads in the longitudinal orientation of fibers, fiber metal laminates are not being used for only tensile properties of them except aramid reinforced fiber metal laminates which response with micro buckling against compression [2].

Table 2.4. Typical Compressive Properties of Glare® Laminates[30].**Table 4**

Properties	Test Direction	GLARE 1		GLARE 2		GLARE 3		GLARE 4		GLARE 5	2024-T3 (1.6 mm thickness)
		2/1	3/2	2/1	3/2	2/1	3/2	2/1	3/2	2/1	
0.2% Compressive yield strength (MPa)	Longitudinal	447	424	390	414	319	309	349	365	283	304
	Transverse	427	403	253	236	318	306	299	285	280	345
Compressive elastic modulus (GPa)	Longitudinal	63	67	69	67	63	60	62	60	61	74
	Transverse	56	51	56	52	62	60	57	54	61	74

0.1

Because of the elasto-plastic behavior of the aluminum composite part of the Glare® faces a catastrophic failure under tensile loads an example of which is shown in Figure 2.8. At first part both materials, aluminum and the composite, responses with their young's modulus and after 250 MPa Aluminum starts to plastically deform so the incline decreased but the fiber metal laminates showed good resistance by the linear elastic response of the composite inside. (Figure 2.9)

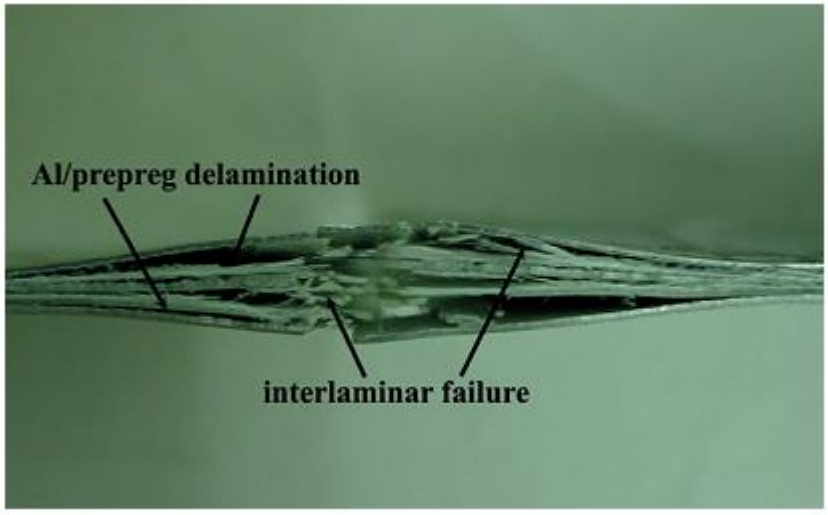

Figure 2.8. Typical fracture pattern for Glare® Laminates Under Static Tensile Loading [3].

Very limited data has been published about crack opening behavior of GLARE® laminates.

An analytical modeling includes in-plane forces, moment results in the composite, mid-plane strains and the curvature may seem like giving well results/almost the same with the experimental results.

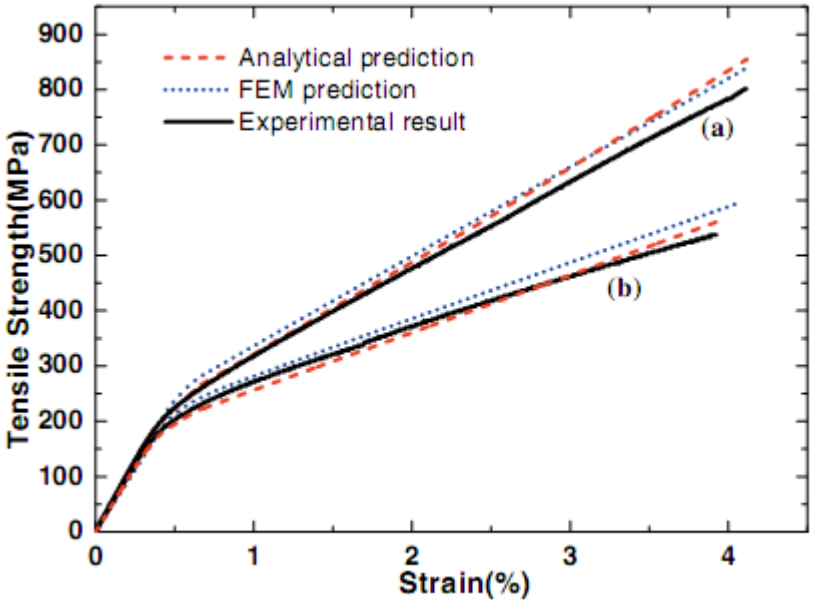

Figure 2.9. Stress-Strain Curves for Glare®4-3/2 under uniaxial tensile loading (a) longitudinal; (b) transverse [3]0.2

By the classical lamination theory the relationship between the applied load and the deformation can be defined as:

$$\begin{bmatrix} \bar{N} \\ \bar{M} \end{bmatrix} = \begin{bmatrix} A & B \\ B & D \end{bmatrix} \begin{bmatrix} \varepsilon^0 \\ k \end{bmatrix} \tag{1}$$

Where, [N]=[N]+[NT] and [M]=[M]+[MT] where N is in-plane force, M is moment results per unit length, ε and k represent the mid-plane strains and curvature, and N and M are thermal force and moment results per unit length respectively.

The resultant forces and moments are obtained by integration of the stresses in each layer over the laminate thickness H;

$$[N, \quad M] = \int_{-H/2}^{-H/2} [\sigma^k](1, z)dz. \tag{2}$$

The stress $[\sigma]^k$ in the kth ply at a distance z, at any distance of loading can now be expressed as;

$$\begin{bmatrix}\sigma_{11}\\ \sigma_{22}\\ \sigma_{12}\end{bmatrix}^k = \begin{bmatrix}Q_{11} & Q_{12} & 0\\ Q_{12} & Q_{22} & 0\\ 0 & 0 & Q_{66}\end{bmatrix}^k \left\{\begin{bmatrix}\varepsilon_{11}^0\\ \varepsilon_{22}^0\\ \varepsilon_{12}^0\end{bmatrix} + z\begin{bmatrix}K_{11}\\ K_{22}\\ K_{12}\end{bmatrix} - \begin{bmatrix}\alpha_{11}\\ \alpha_{22}\\ \alpha_{12}\end{bmatrix}\Delta T\right\}, \quad (3)$$

Where Q_{ij} is the reduced stiffness matrix, αij is the ply lamina coefficient of thermal expansion in the principal material coordinate system and ΔT is the temperature change during curing.

Under a uniaxial load, the deformation behavior of the laminate, as glare® has been accepted that all layers experience the same deformations because of compatibility of all of the layers, is described by the relation;

$$[dN]=[A][d\varepsilon] \quad (4)$$

Where dN is the increments of the in-plane force per unit length, dN=Hdσ and H is the total thickness of the fiber metal laminate. The extensional stiffness matrix [A], coupling stiffness matrix [B] and bending stiffness matrix [D] must be identified as;

And the extensional stiffness matrix [A] can be calculated as;

$$[A]= n^{A1}[Q^{A1}]h^{A1}+n^{c}[Q^{c}]h^{c} \quad (5)$$

Where the number and thickness of the aluminum layer and glass/epoxy composite layer are expressed as n^{A1}, h^{A1} and n^c, h^c respectively.

The composite in the glare® laminate can be accepted as linear elastic orthotrophic material. Stress-strain relations according to increments are;

$$[d\sigma^c]=[Q^c][\, d\varepsilon^c] \quad (6)$$

Where Q^c is the reduced stiffness matrix of composite layers.

$$[Q^c] = \begin{bmatrix} \frac{E_{11}^c}{1-v_{12}^c v_{21}^c} & \frac{-v_{12}^c E_{22}}{1-v_{12}^c v_{21}^c} & 0 \\ \frac{-v_{12}^c E_{22}}{1-v_{12}^c v_{21}^c} & \frac{E_{22}^c}{1-v_{12}^c v_{21}^c} & 0 \\ 0 & 0 & G_{12}^c \end{bmatrix} \quad (7)$$

After the point of yielding, aluminum shows great plasticity so, Glare® laminates show nonlinear tensile response. To handle accurate elastic analysis for accurate prediction of stress-strain relation; as using the 2024 T3 aluminum alloy is being taken as the aluminum, the plastic flow potential for the plastic deformation of aluminum was taken as;

$$f^{A1}(\sigma_{ij}) = 1/2[b_{11}(\sigma_{11})^2 + (\sigma_{22})^2 - \sigma_{11}\sigma_{22} + 3(\sigma_{12})^2] \quad (8)$$

The plastic strain increments $(d\varepsilon p)_{ij}$ are belonged to the stresses by the potential flow rule;

$$(d\varepsilon_p)_{ij} = d\lambda(\partial f^{A1} / \partial \sigma_{ij}) \quad (9)$$

A power law relates the effective stress and the effective plastic strain; for A1

$$\acute{\varepsilon}_p = \varphi(\sigma')^{\gamma} \quad (10)$$

where the effective stress is defined as: $\sigma' = (3f)1/2$

$$d\lambda = 3/2.\ (d\varepsilon_p' / \sigma') = \Omega(n_1 d\sigma_{11} + n_2 d\sigma_{22} + n_3 d\sigma_{33}) \quad (11)$$

where, $\Omega = (9/4).\ \Phi\gamma.\ (\sigma')\gamma - 3$, $n_1 = 0{,}5(2b11\sigma11 - \sigma22)$, $n_2 = 0{,}5(2\sigma22 - \sigma11)$, $n_3 = 3\ \sigma12$ for Al.

Combining the equation (11) with (8) and (9), the relations between plastic strain increments and the stress increments are obtained;

$$[d\varepsilon_p]=[S_p][\ d\sigma] \text{ for Al} \tag{12}$$

Where Sp are given by;

$$\begin{aligned}
(S_p)_{11} &= \Omega.\ n_1\ n_1 \\
(S_p)_{12} &= \Omega.\ n_1\ n_2 \\
(S_p)_{16} &= \Omega.\ n_1\ n_3 \\
(S_p)_{22} &= \Omega.\ n_2\ n_2 \\
(S_p)_{26} &= \Omega.\ n_2\ n_3 \\
(S_p)_{66} &= \Omega.\ n_3\ n_3
\end{aligned} \tag{13}$$

For the elastic part of the aluminum, the stress – strain relation is;

$$[d\varepsilon_e]=[S_e][d\sigma]. \tag{14}$$

Where S_e;

$$[S_e^{Al}] = \begin{bmatrix} \frac{1}{E^{Al}} & \frac{-v^{Al}}{E^{Al}} & 0 \\ \frac{-v^{Al}}{E^{Al}} & \frac{1}{E^{Al}} & 0 \\ 0 & 0 & \frac{1}{G^{Al}} \end{bmatrix} \tag{15}$$

From the equations (12) and (16) we can get the total incremental stress-strain relation of the aluminum layers;

$$[d\varepsilon]= [d\varepsilon_e]+ [d\varepsilon_p]=([S_e]+[S_p])[d\sigma]. \tag{16}$$

So for the aluminum;

$$[d\sigma]=[Q][d\varepsilon], \tag{17}$$

where

$$[Q]= ([S_e]+[S_p])^{-1}. \tag{18}$$

When the equation (20) is combined with equations (5) and (4), a total incremental constitutive relation is obtained:

$$[dN]=[\, n^{A1}h^{A1}([S_e]+[S_p])^{-1}+n^{c}h^{c}(Q^{c})] \tag{19}$$

Now the equation (19) can be used to handle the stress – strain relationship of Glare® laminate when combined with equations (15), (13), (7) and (3) [3].

Table 5

Table 2.5. Applied property parameters of all constituents in Glare® laminates for prediction.

Materials	E_{11} (GPa)	E_{22} (GPa)	G_{12} (GPa)	$\sigma_{0.2}$ (MPa)	$E_{plastic}$ (MPa)	ν_{12}	$\alpha_{12} \times 10^{-6}$ (°C^{-1})
2024-T3 aluminium	72	72	26.6	350	887	0.33	22
Glass fibre	86	86	32.3	/	/	0.33	5.2
Epoxy	3.4	3.4	1.26	/	/	0.35	60

Stiffness and fracture analysis of composites/fiber metal laminates must depend on different kinds of loadings, dynamic state, cracks in the resin which are parallel to the reinforcement and in the off-axis ply is the beginning of the all interlaminar failures [49].

It can be seen that fatigue resistance of a fiber metal laminate with a fatigue crack initiation is greater than a fiber metal laminate that has a saw cut due to the unbroken fibers and narrower delamination zone around the crack which effects the strain length

of the fibers very high. The post impact resistance of a fiber metal laminate gives excellent results which is the main aim below damage tolerant inspection logic [50]. Blunt notch resistance of GLARE® is superior to ARALL® because of high ultimate strength of glass and high strain to fracture of glass when the properties of GLARE® materials with their volume fraction-fiber directions are optimized against the size and the shape of the flaw averages[51].

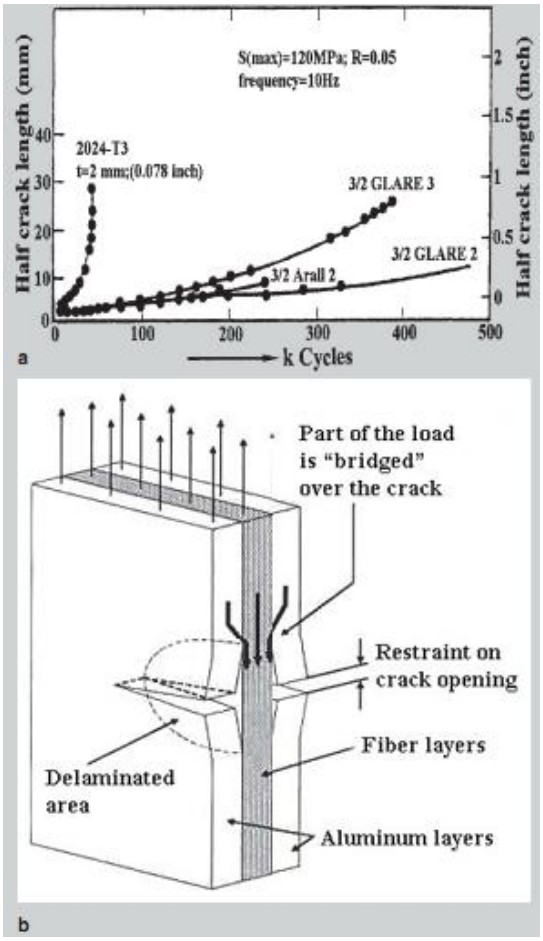

Figure 2.10. The Fatigue Behavior of Glare® (a) Fatigue Crack Growth behavior of Glare® for a fuselage loading; (b) a Schematic of Fatigue-Crack Mechanism [30].0.3

With a saw cut flaw fatigue behavior comparison between monolithic aluminum and different kind of glare® laminates. As can be seen from figure 2.19 glare® laminates show excellent fatigue behavior with linear and slow crack propagation. By crack

bridging a significant load is being carried by the fibers, stress intensity factor and the crack growth rate in the aluminum layers are being decreased [52].

To understand the crack growth mechanism in fiber metal laminates better, the bridging tractions must be determined as a function of delamination shape which is being effected by lay-up procedure, adhesion shear according to inter laminar stresses and crack size and geometries [51]. Matrix micro cracks start to initiate long before than composite material loses its' loading and load transferring capacity. Matrix cracks reduce stiffness and strength of the material, changes the thermal coefficient of expansion, moisture absorption and natural frequency of the composite [49].

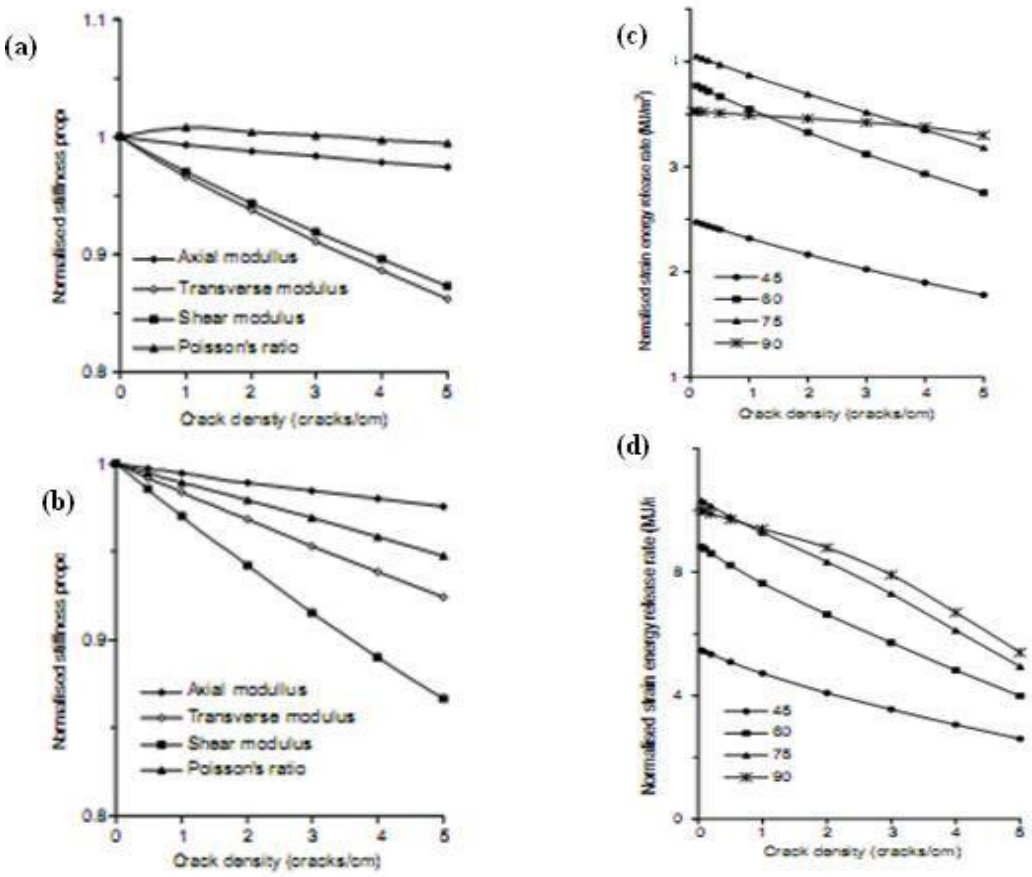

Figure 2.11. (a)(b) Normalised Stiffness Properties of graphite epoxy laminates as a function of crack density (c)(d) Strain Energy Release Rate for matrix cracking as a function of crack density. 0.4

High failure strain and high strain strengthening of fibers are giving to the glare® highest performance about impact resistance.

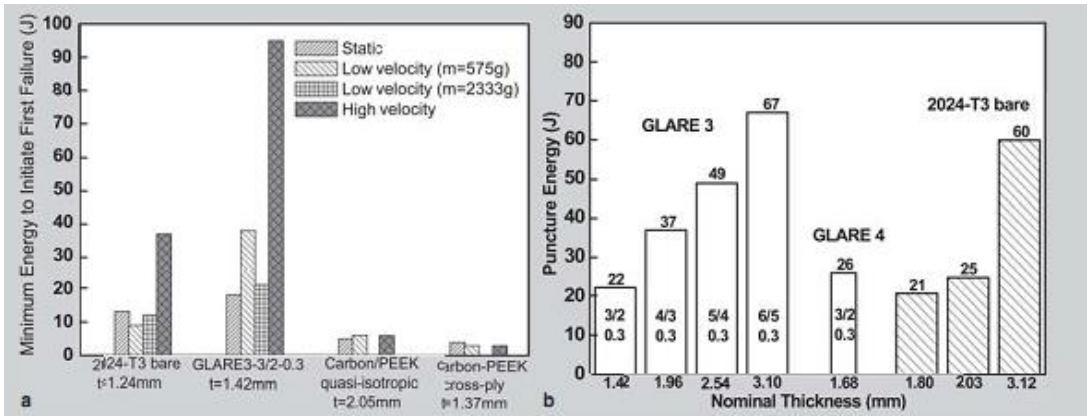

Figure 2.12. The impact behavior of Glare® (a) Comparison of impact performance of Glare® 3 and other aerospace materials; (b) Low velocity impact performance of cross plied Glare® Laminates [30].0.5

At relatively low speeds of aircraft, impact tolerance of both monolithic aluminum and the fiber metal laminates are the same but at the high speed levels because of the fibers' strain hardening and the strain rate of aluminum, fiber metal laminates show extremely better results.

After the impact, the damage can be seen as a dent on the aluminum layer of glare® and there is a very small damage distributed in-plane of the fiber metal laminate compared to the other composites. The "compaction after impact" test results are the same with the monolithic aluminum and there is no buckling of delamination inside the sandwich structure of the glare® which is very important for composites too.

Table 2.6. Post impact fatigue test results of Glare® [30].

Materials	E_{impact} (J)	Cycles to Initiation	Cycles to Failure
GLARE 4	54	37,500	61,200
GLARE 5	46	48,000	71,750
GLARE 5	36	30,000	84,000 impact fatigue
Aluminum 2024-T3	58	No visible cracks, sudden failure	25,500

By the development of “splicing concept” bigger panels of fiber metal laminates could have been manufactured which gave us inspiration to imagine to fabricate the fiber metal laminates with holes just seem like gaps that filled with epoxy primers between splices.

2.7. Wetting Analysis

One of the most important parameter influencing the strong durable bonded structures is wetting of the liquid over a substrate.

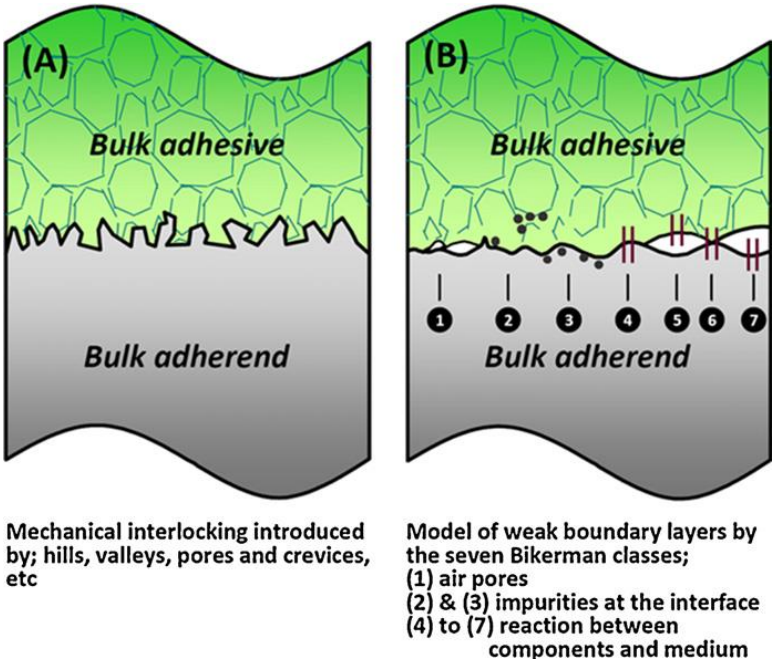

Figure 2.13. Interface between adhesive and substrate (a) contaminant and void free, (b) contaminated [10].

Figure 6

The surface must be free from contaminants and impurities must have good topography to ease the wetting and to ban to create voids, surfactants on the surface which are undesired must be removed and the surface must let the optimum wetting conditions between the liquid and the solid as they react to bond each other. The microstructural composition of the interface needs attention a lot why it carries multidisciplinary engineering knowledge such as bulk properties, surface features, chemistry of the both sides, gradients of the treated surface etc [15].Porosity effects the loading response of the composite structure very bad especially on the inter laminar shear strength [12].

"Wetting of a liquid over a solid" phenomena still does not fully understood because of some hard issues about the problem.

- Contaminants and physical modification of the surface makes it very sensitive,
- Measurements are not so easy even for very high technological capabilities,

- Young and Laplace approximations are very newly started to be understood [17].

The physicochemical situation of the thermodynamic wettability of the substrates clarified by different scientists but the changes of the thermodynamic equilibrium still needs serious effort [53].
Surface energies of adhesive, aluminum substrate and interface between them can be analytically calculated from contact angle measurements[54].

When a liquid drop put in contact with a flat substrate, it shows different kinds of behaviors as shown in figure.1, partial or complete wetting.

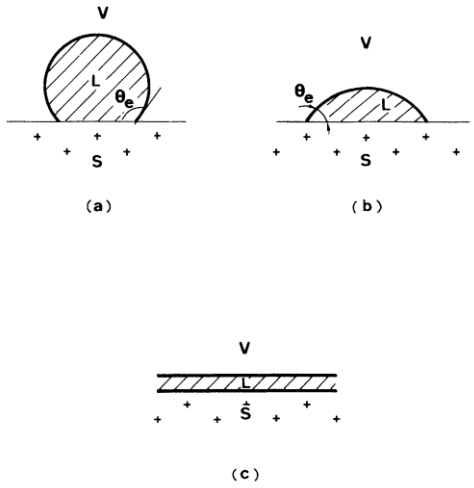

Figure 2.14. Different types of contact angles[55].0.7

Three phases are in contact at the line $\mathcal{L}$; solid, liquid and the equilibrium vapor. The principle that the British scientist Thomas Young declared that, the energy of the drop and the contact angle on the triple line $\mathcal{L}$, does not change with respect to any change of the distance (dx) which may include an increase of the area of the interface.

$$\gamma_{SV} - \gamma_{SL} - \gamma\cos\theta = 0 \qquad (20)$$

Calculating the surface energy according to Gibbs (G) or Helmholtz(F) free energy which needs very precise measurements over solid substrate surfaces, is not possible so we admit surface tension of the substrate as the surface energy [54]. By many experiments it's improved that surface tension of the liquid equals to surface energy of the liquid.

$$\gamma \approx \gamma_{LV} \tag{21}$$

To handle the optimum wetting, surface tension of the liquid must be low enough.

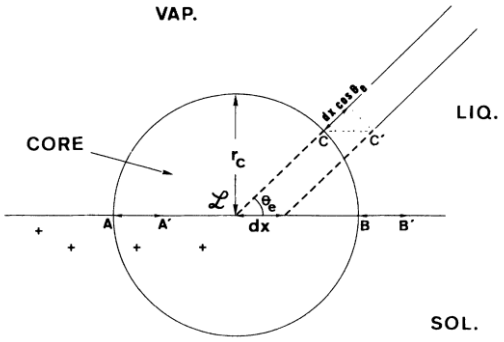

Figure 2.15.Displacemnet of triple line point.0.8 [17]

Young's formulas derivation for the surface energy of the drop:

$$E=\Sigma_{lv}.\ \gamma_{lv}+\Sigma_{sl}.\ \gamma_{sl}+(\Sigma_s-\Sigma_{sl})\ \gamma_{sv} \tag{22}$$

$$E=A_{lv}.\ \gamma_{lv}+A_{sl}.\ \gamma_{sl}+(A_s-A_{sl})\ \gamma_{sv} \tag{23}$$

A_s= Total surface area of the solid, Σ_{lv}=Total area of the liquid-vapor interface respectively [56].

Contact angle can be obtained by;

- Photograph,
- Deflection of rays,

- Interferential Techniques,
- From the rising motion of the capillary in a columnar height [17].

Special Features of Complete Wetting;

Complete wetting occurs when the contact angle equals to zero.

$$\text{If } \theta=0, \text{ then, } \cos\theta=1, \text{ so } \gamma_{SV-}\gamma_{SL}=\gamma.$$

$\gamma+\gamma_{SL}$ cannot be larger than γ_{SV} because if they'd be larger, it means that the surface energy of the substrate changes with the liquid so the phenomena would not be wetting at thermodynamic equilibrium. So it can only be an equation that ;

$$\gamma_{SV}=\gamma_{SL}+\gamma \tag{24}$$

for the complete wetting. In nonequilibrium conditions spreading coefficient characterizes the wetting because of the solid/vapor interfacial energy is bigger than $\gamma_{SL}+\gamma$.

Spreading coefficient is; S.

$$S=\gamma_{SV}-\gamma_{SL}-\gamma \tag{25}$$

and if S is large positively, it favors the spreading. When the spreading coefficient is bigger than zero, S>0, resin will be spread over the aluminum substrate.

Our substrate is in the classification of the hard solids with high energy surfaces.

Surface energy determination also associated with failure and creating new surfaces according to creation of new surfaces with the work of adhesion (W_a) and work of cohesion (W_c);

$$W_a=\gamma_1+\gamma_2-\gamma_{12} \tag{26}$$

$$W_c=2\gamma_1 \tag{27}$$

Roughness may increase the interfacial bond and fracture energy of the surface. Wenzel roughness factor can be calculated by surface roughness profilometry.

Wenzel roughness factor;

$$r=A/A_0 \quad (28)$$

This approach assumes that there is no chemical difference between as received aluminum and the roughened surface respectively. For fine surfaces, where the roughness decrease, Wenzel's roughness factor cannot be admitted as a convincing realistic determination function, just because the roughness increases the entropy of the substrate surface and brings the two phases together [54].
Texturing the surface of the solid changes the contact angle as a function of the wettability of the substrate [57].

When a substrate surface roughened, roughness factor can be used as;

$$Cos\theta_{rough}=r.\ Cos\theta_{smooth} \quad (29)$$

With the roughness factor, r, spreading coefficient can be held;

$$S/\gamma_2=r(\gamma_{LV}-\gamma_{12})/\ \gamma_2-1 \quad (30)$$

Means that if $\gamma_{LV}-\gamma_{12} > 0$, than $\theta_{smooth}<\pi/2$ and roughening the surface increase the tendency for the spreading. If $\theta_{smooth}>\pi/2$, then the opposite occurs, and spreading efficiency decreases [54].

Hysteresis of the Contact Angle: Two sides of the drop shows different contact angles. It happens because surfactants which the liquid carries and the inhomogeneity of the surface of the solid changes the mass balance of the drop. [56,58].While the drop of liquid improves on a solid surface, because of the motion of itself, the drop loses its' shape of semi-sphere but gains a shape with a larger contact angle in the head and smaller contact angle in the back. Wetting will happen when the contact angle goes to zero according to Young's rule. But impregnation occurs when the contact angle is smaller than 90°. During resin infusion we need to impregnate the surface of

aluminum, so the contact angle results show that the sand brazing, silanization samples of our substrates gives the range in the impregnation zone [56]. The forehead angle is the advancing contact angle and the other is the receding one respectively.
There can be an asymmetry created between the different edges of the drop according to be the edges stay on hydrophobic or the hydrophilic sites of the substrate [57].
The sessile drop contact angle we have measured in Atılım University facilities carries a triple line point, $\mathcal{L}$, that is immobiled/pinned not with $\theta=\theta_e$ but in an interval that;

$$\theta_{receding} < \theta < \theta_{advancing}. \quad (31)$$

$\theta_{advancing}$: can be measured when spreading positively enlarges and, $\theta_{receding:}$ can be measured when the liquid shrinks.

The sources of hysteresis are; Surface roughness, Chemical contaminations, Solutes in the liquid [17]. Trillat and Fritz (1937) showed that, $\mathcal{L}$ is easily pinned when parallel to the grooves on the surface with the roughness.

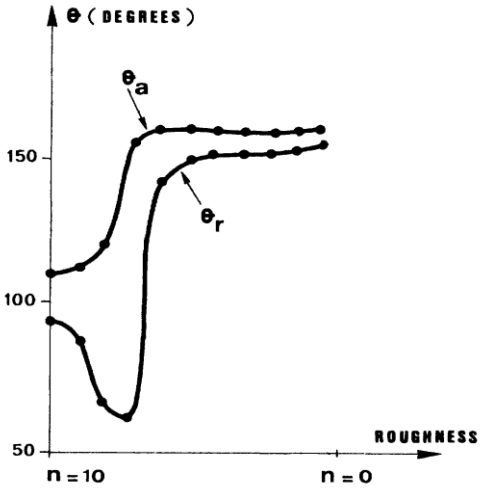

Figure 2.16. Advancing and receding contact angle versus roughness [17].0.9

Figure shows that contact angle hysteresis vanishes at the point where the advancing and receding angles variation goes parallel. Bu t because we make vacuum infusion

the process itself pushes the liquid drops through the outlet, we can neglect this phenomenon. So contact angle & roughness figure gives us how the contact angle changes. When we come to a smoother surface, θ_r jumps in the second interval from n=0 to n=10. On the rough side θ_r and θ_a are parallel. So we made roughening by sand papers with parallel motions.

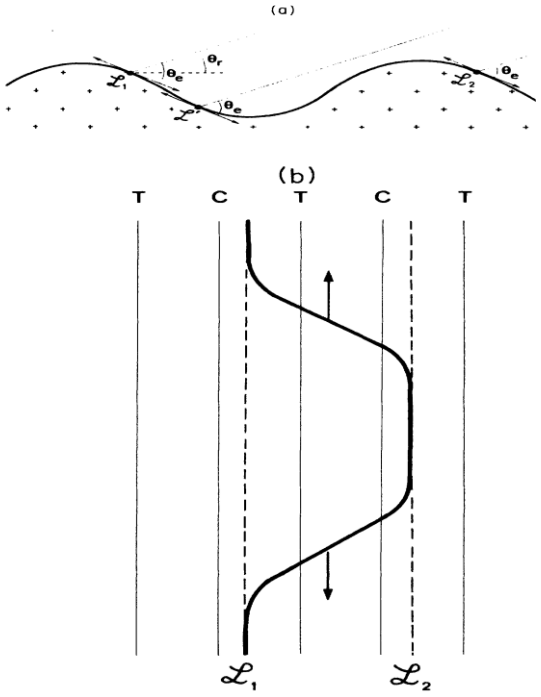

Figure 2.17. Triple line point through grooves [17].0.10

If the grooves are too deep, vapor can be entrapped through the troughs and covered by the liquid. When the triple line shows an angle to the grooves, there is no pinning that occurs and $\mathcal{L}$ proceeds. Because of sand papers have random arrangement of their own grids; during resin infusion resins' way under the negative pressure creates an angle with the rough surface topography of our aluminum substrate.

The energy change when the liquid changes its position can be predicted as;

$$dE=r(\gamma_{sv}-\gamma_{sl})dx+ \gamma_{lv}.dx.\cos\theta^{*} \quad (32)$$

$$\cos\theta^{*}=r.\ \cos\theta,\ (\cos\theta^{*}=\mathrm{Cos}\theta_{rough}) \quad (33)$$

For a roughened surface of aluminum, during resin improves through outlet of the resin infusion set-up, it's desirable to achieve that the resin smoothly follows the roughness of the substrate. At every rough site of the surface, u_L and u_S changes dramatically which are liquid and solid depth and height modulations.
For a very randomly roughened surface it's not possible to measure these depth/height changes which brings us the energy of the film that is desired as;

$$E=\int dA[W(h+u_L+u_S)+1/2.\gamma_{LV}.(\nabla u_L)^2] \quad (34)$$

Where dA is the change in the area during propagation, h is the thickness of the film. W is the Van der Waal forces that belongs the thickness of the film as;

$$W(h)= - A/12\pi h^2 \quad (35)$$

Where A is the Hamaker constant which related to the contrast in polarizibility between the metal substrate and the resin. At the rough hills, there must be solution about the hemi-wicking sites of Wenzel's scenario, which rules that the liquid wets the tops of the hills but not the valleys. The area of the tops of the hills would need to handle the fraction of the hills area over substrate area (Ø) will be needed to actual contact angle with;

$$\cos\theta^*=(1- Ø)+ Ø_S \cos\theta \quad (36)$$

to handle the energy change during the contact line displacement which creates an energy change with different possibilities of wetting hills and crevices with;

$$dE=[f_1(\gamma_{sl}-\gamma_{sv})_1+ f_2(\gamma_{sl}-\gamma_{sv})_2]dx+ \gamma_{lv}.dx. \cos\theta^* \quad (37)$$

where f_1, f_2 are the probabilities. Another question maker situation is the contact angle hysteresis calculation. Because the roughness does not include an arbitrary chase, for one hill made calculation cannot take us to overall estimation of the contact angle hysteresis of the resin drops over the all surface of the substrate [56].

Equilibrium considerations gives the details of roughness determine the wetting of roughened substrate surface with a liquid.

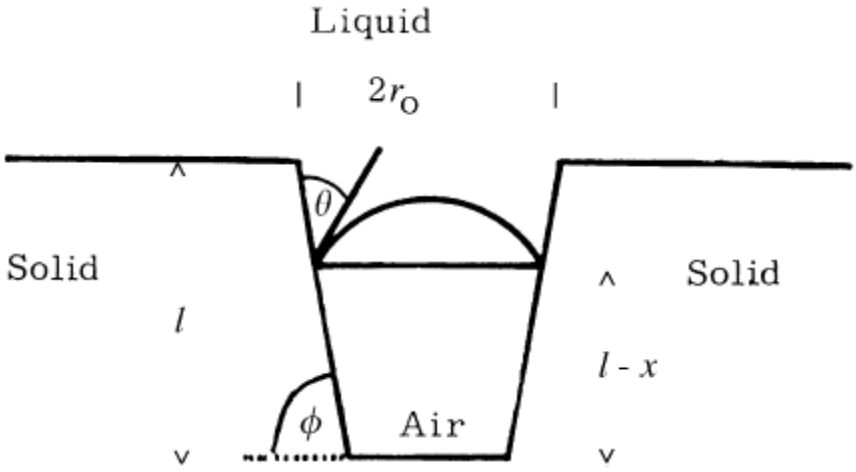

Figure 2.18. Capillary pressure identification in a small pour [54].0.11

Penetration to a modeled pore with sizes shown in figure 2, occurs when the pressure of the air inside the pore balances the capillary pressure [59]. This capillary pressure for a pore is;

$$\text{Capillary Pressure}=2\,\gamma 2.\sin(\theta+Ø)/(r_0\text{-x.cot }Ø) \quad (38)$$

If $(\theta+Ø) <180°$ then penetration occur.

$$x=l(1-(Pa.r/2.[2\,\gamma_2\cos\theta+Pa.r]) \quad (39)$$

means smaller pore gives possibility for penetration [54].

CHAPTER 3

EXPERIMENTAL PROCEDURE

3.1. Materials

Resin infusion process is one of the composite manufacturing processes used in different industries, most frequently aviation, naval architecture, railways, component manufacturing, automotive etc.

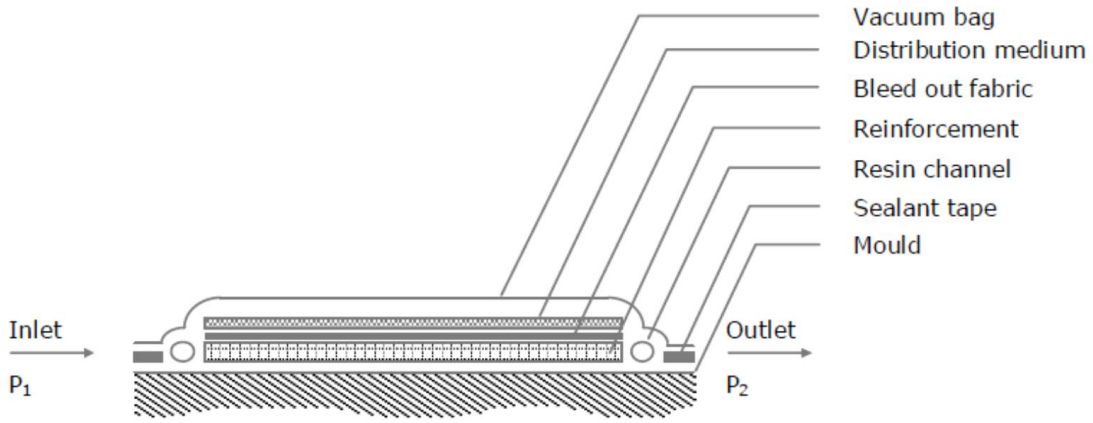

Figure 3.1. Typical resin infusion set-up [13].0.1

Resin infusion process is a dynamic resin flow process which wets the preform under the mold with negative pressure sucked from the outlet of the mold. Contamination caused by the consumables used and void content captured within the mold is critical in terms of the mechanical behavior of the final product near the optimum wetting. Although the resin flow can be observed from the top, transverse and in-plane flow of resin needs to be optimized during labor and set-up planning.

While prepreg-autoclave processed composites reveal the best mechanical performances because of the low void content-under %2- under the impregnation spreading is more efficient than other composite manufacturing techniques, it is a long batch and relatively expensive production method. So the best candidate to replace prepreg-autoclave process is Resin or Resin Infusion process. Lowering the void content and improving the wetting of the preform under the mold are going to make the resin infusion first choice of the industries with its cheap manufacturing consumables and process. Until now, there is no application that tried out resin infusion technique for fabricating fiber metal laminated composites.

The consumables used during resin infusion process are as follows;

- Resin
- Resin Hardener
- Sealing Tape
- Vacuum Bag
- Mold Releasing Paste
- Aluminum 2024 T3
- Glass Fiber
- γ-glycidoxytrimethoxy silane
- Sand Paper: 180, 240, 1000
- Pure water, ethanol, toluene
- Peel ply
- Perforated
- Vacuum pump

- Hoses-normal, scratched
- Tri-gate junction for resin flow

3.1.1. Resin

During resin infusion process Hexion Epikote^{TM} MGS LR-160 was used as the Bisphenol A-epichlorohydrin resin. As resin infusion necessitates very low viscosity resin, LR-160, which has been widely used in such kind of applications in aerospace and in the other industries, was selected.

Some tag properties of the resin are given below:
Approval: German Federal Aviation Authority
Boiling Point > 200 °C
Flash Point > 150 °C
Vapor Pressure < 0.14 hpa
Density at 20 °C= 1.13-1.17 g/cm^3
Solubility in / Miscibility with water: not miscible or difficult to mix
Viscosity dynamic at 25 °C= 700-900 MPa*s

3.1.2. Resin Hardener

With Hexion Epikote^{TM} MGS LR-160 resin Epikure^{TM} Curing Agent MGS LH 160 (3-aminomethyl-3,5,5-trimethylcyclohexylamine) was utilized. Resin and hardener set used in this study is shown in Figure 3.2.
Boiling point : > 200 °C (392 °F)
Flash point : > 100 °C (212 °F)
Density : ca. 0.960 g/cm3
Solubility in water : insoluble
Viscosity : Dynamic- 10 - 50 mPa·s 25 °C

Figure 3.2. Resin and hardener used in this study.0.1

3.1.3. Sealing Tape

While vacuuming the mold, Umeco brand sealant tape enables the air tightness. Surrounding the mold with the sealant tape and sticking it to the vacuum bag, the mold will stay under the vacuum properly to handle the negative pressure during the resin flow. Sealant tape used in this study is shown in Figure 3.3.

Figure 3.3. Sealant tape used in this study.0.1

3.1.4. Vacuum Bag

It enables the proper vacuum environment with sealing tape. Different than the currently applied procedure, there are some applications where two layers of vacuum bag or vacuum bags for special temperature intervals etc are used. Beside these, to handle some special surfaces, there are variety of vacuum bags which have porous surface for different roughness. The vacuum bag used in this study is shown in Figure 3.4.

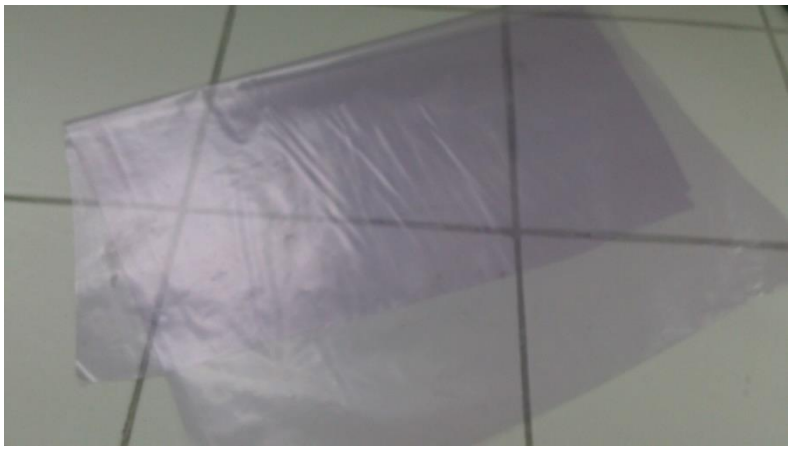

Figure 3.4. Vacuum used in this study.0.1

3.1.5. Mold Releasing Paste

This product is being smeared gently to the surface of the mold to separate the surface properly after the curing of the resin. The product shown in Figure 3.5 was used in this study as its application is easier than that of other mold releasing pastes.

Figure 3.5. Releasing paste used in this study.Figure 2

3.1.6. Aluminum 2024 T3 Alloy

Typical characteristics of the aluminum alloy used in this study (Figure 3.6) are as follows:

Ultimate Tensile Strength:	426 - 431 MPa
Yield Strength:	288 - 292 MPa
Elongation:	% 12.5-%16.5
Thickness:	0.5 mm

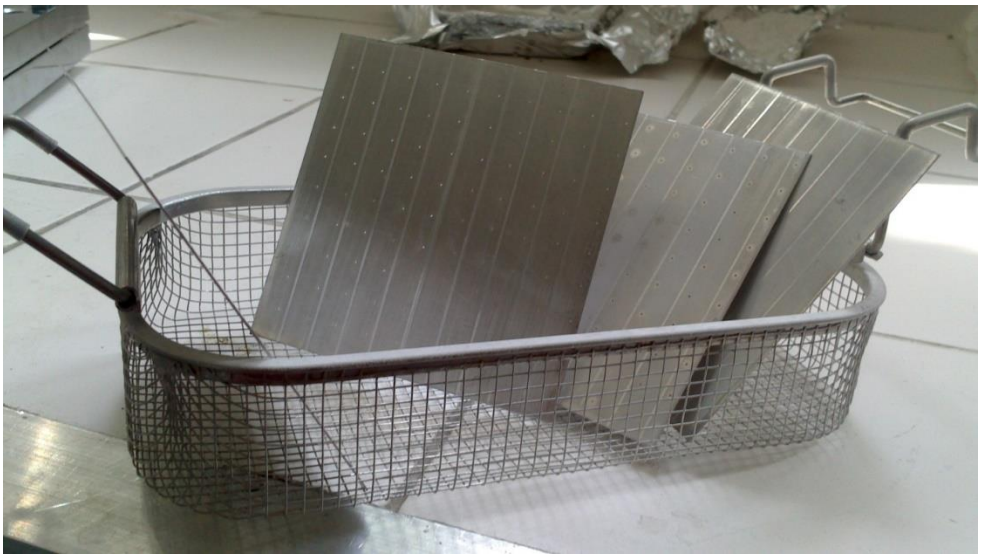

Figure 3.6. 2024 T3 Aluminum alloy sheets used in this study.0.1

3.1.7. Glass Fiber

0/90 degrees oriented, 1/3 cross plied-EC5/11×2 tex, C class glass fiber woven fabrics with areal weight 105 g/m^2 were used in this study. Typical characteristics of the glass fiber woven fabrics used (Figure 3.7) are as follows:

Thickness (43%): 0.13 mm
Tensile Elastic Modulus: 19 GPa for both the elastic and the shear modulus
Tensile Strength: 335 MPa
Compressive Strength: 355 MPa
Inter laminar Shear Strength: 45 MPa
Torsional Strength: 495 MPa

Figure 3.7. Glass fiber woven fabrics used in this study.Figure 2

3.1.8. Silane Coupling Agent

In order to prepare the silane solution 95 vol% Ethanol and 5vol% pure water solution was prepared, and its pH was kept between 4.5-5.5 by acetic acid addition. 0.7 wt% γ-glycidoxytrimethoxy silane was added to the prepared alcohol-water solution. After the aluminum surfaces were prepared with proper-contamination free-activated sand paper and cleaned ultrasonically, the silane solution was sprayed to a single face of the

aluminum surfaces. During the silane treatment of the aluminum surfaces a Lotus AS18-2 vacuum pump with a very small diameter spraying nozzle was utilized (Figure 3.8). After silane solution was sprayed at 0.15 bar pressure, the aluminum sheets were held at 110 °C for at least 1 h.

Figure 3.8. Spraying of the prepared silane solution to the aluminum surfaces.0.1

3.1.9. Sand Paper

To achieve aluminum surfaces with controlled macro roughness, 180-240 and 1000 sand papers were used (Figure 3.9). In the case of aluminum surfaces containing grooves and holes, only 1000 grid sand paper was used. On the aluminum samples without grooves and holes, 180 or 240 grid sand papers were preferred to get more roughened surface to increase the wetting – adhesion area.

Figure 3.9. Sand papers used in this study.0.1

3.1.10. Pure Water, Ethanol, Toluene

While cleaning all of the parts being used during the experiments and sample preparations, pure water and ethanol have been used. After sand paper abrasion and ultrasonic cleaning of the aluminum parts, their surfaces have been cleaned with a toluene soaked lint free towel.

3.1.11. Peel Ply

Peel ply (Figure 3.10) was used to remove the material after the completion of the curing from the perforated, vacuum bag, breather, flow mesh and surface modifier.

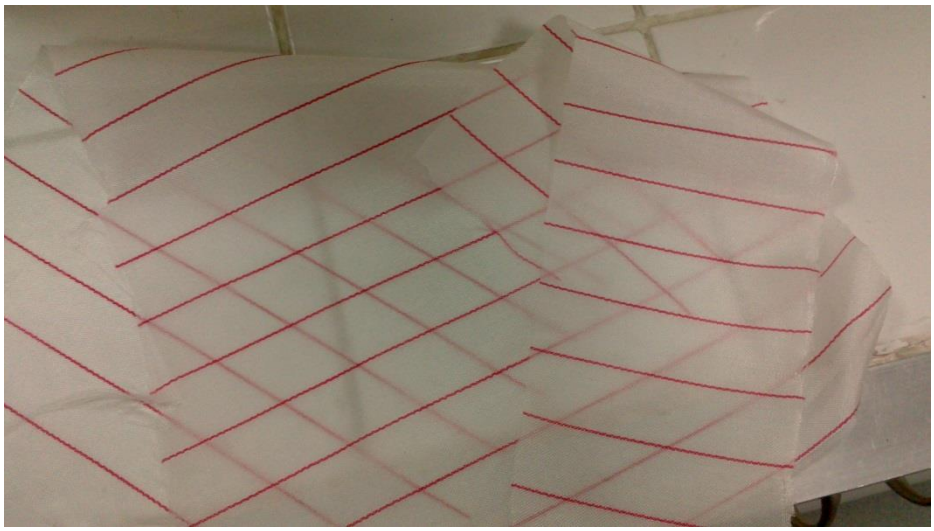

Figure 3.10. Peel ply used in this study.0.1

3.1.12. Perforated

During the infusion process, perforated (Figure 3.11) takes the excess resin from the mold through its holes like a jack-valve operating system without letting the resin to flow backwards. Perforated was used both after and over the peel ply.

Figure 3.11. Perforated used in this study.0.1

3.1.13. Breather and Flow Mesh

Breather is being used to get the excess resin which differs from the perforated by its cotton like structure which sucks and holds the excess resin. Flow mesh is being used to make the resin to reach to the end of the mold faster. Decreasing the infusion time is important because of the limiting resin-end product and product dimensions in some applications.

3.1.14. Vacuum Pump

During resin infusion process a Telstar 2F9 vacuum pump (Figure 3.12) was used to create 0.7 bar negative pressure in the mold.

Figure 3.12. Vacuum pump utilized in this study.0.1

3.1.15. Hoses: Normal-Scratched

Normal hoses with different inner-outer radii have been used to suck the air by the pump on the outlet of the mold side and to suck the resin at the inlet of the mold. Scratched hoses have been used to separate the resin at the inlet through the width of

the mold and to take out the excess resin gathered at the outlet of the mold (Figure 3.13).

Figure 3.13. Hoses: Scratched-Normal used in this study.0.1

3.1.16. Brass Tri-Gate Junctions

To take out the gathered air and resin out of the mold at the outlet and to let the resin in at the suction side, tri-gate junctions made of brass have been used.

3.2. General Procedure

Fabrication of the fiber metal laminates via resin infusion starts with the surface modification of the aluminum layers. Before the surface treatments, all of the aluminum layers were cleansed with ethanol. Applied surface modifications show variation for different samples. Some horizontally resin infusion applied samples contain aluminum layers with the grooves and holes introduced. The other samples have been roughened with sand papers with the proper grids. Aaluminum surface preparation was finalized by cleaning the layers with ultrasonic cleaner and toluene degreasing. Contact angle measurement has been conducted on different tailored surfaces of aluminum substrates.

Resin infusion set-up preparation continued in parallel with the aluminum layer enhancements. Following the silane treatment of the aluminum surfaces, the bench for

composite manufacturing, process set-up, consumables according to sample sizes, fibers and the other devices/materials were prepared for resin infusion.
After resin infusion, x-ray photos of some parts have been taken to see the hole arrangement of the fiber metal laminate sample. Following this step, samples were sliced for three-point bending test according to DIN EN 2563 using Isomet-5000 Micro Cutter.

After the three-point bending tests, observations of the results according to different modifications, evaluation of the samples and their surfaces according to fracture and wetting considerations have been conducted. SEM photos have been taken to see and to compare the fracture surfaces of different samples of fiber metal laminated composites fabricated by resin infusion.

In order to make comparison, sand paper and silane treated aluminum samples have been united with prepreg material those have been produced by Odak Composites/OSTIM to fabricate the fiber metal laminated composites using hot-pressing.

3.3. Sample Preparation

3.3.1. Aluminum Layer Preparation

The aluminum used in this study is cladded 2024 T3 alloy which is being used especially in aerospace industry, therefore procured from TAI - Turkish Air Industries specially. The characteristics of the 2024 T3 aluminum alloy have been given in the earlier sections.

Aluminum parts have been sliced to (10 cm X 10 cm) pieces in TAI facilities. According to DIN EN 2563, three-point bending test specimens must be of size 1 cm X 10 cm, so 10 cm X 10 cm samples have been fabricated and 3 mechanical testing specimens were taken out from their central section.

To get the maximum wetting during fabricating fiber metal laminated composites with horizontal resin infusion, aluminum substrate surfaces were modified with holes and grooves. Holes have been used to wet the inner parts of the mid-range/second and third layers out of the four aluminum layers of the fiber metal laminated composite. The arrangement of the holes changed for different samples to see and compare the results of the inter laminar shear stress resistances of the laminates. In Ergül Makine/OSTIM facilities, holes have drilled according to the hole arrangement of the sample series. Drilling has been made with drilling machine by using needle driller at 2400 rpm/min (Figure 3.14). The radius of the holes is 0.8 mm and was held constant through all of the parts. To power this intra laminar motion of the resin through the holes and to ease the triple line point chase on the surfaces of the aluminum laminates grooves have been used. In the same facilities grooves have been drawn to the surface of the layers using a manual apparatus which has been adapted for this study.

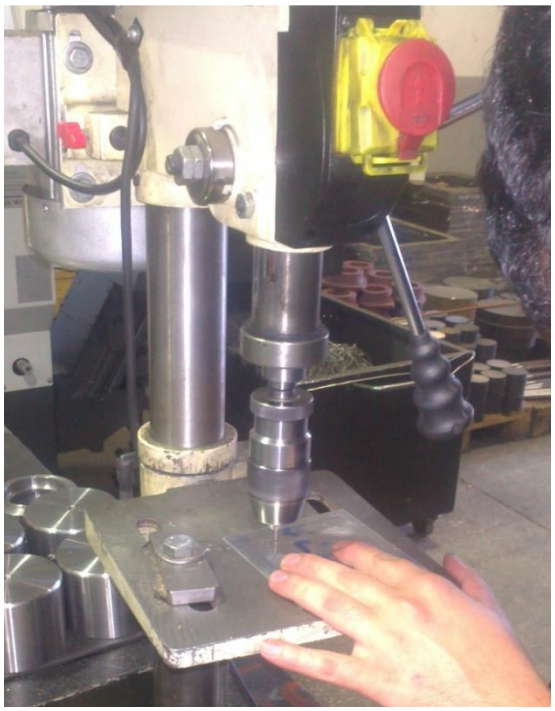

Figure 3.14. Drilling of holes on 2024 T3 aluminum alloy.0.1

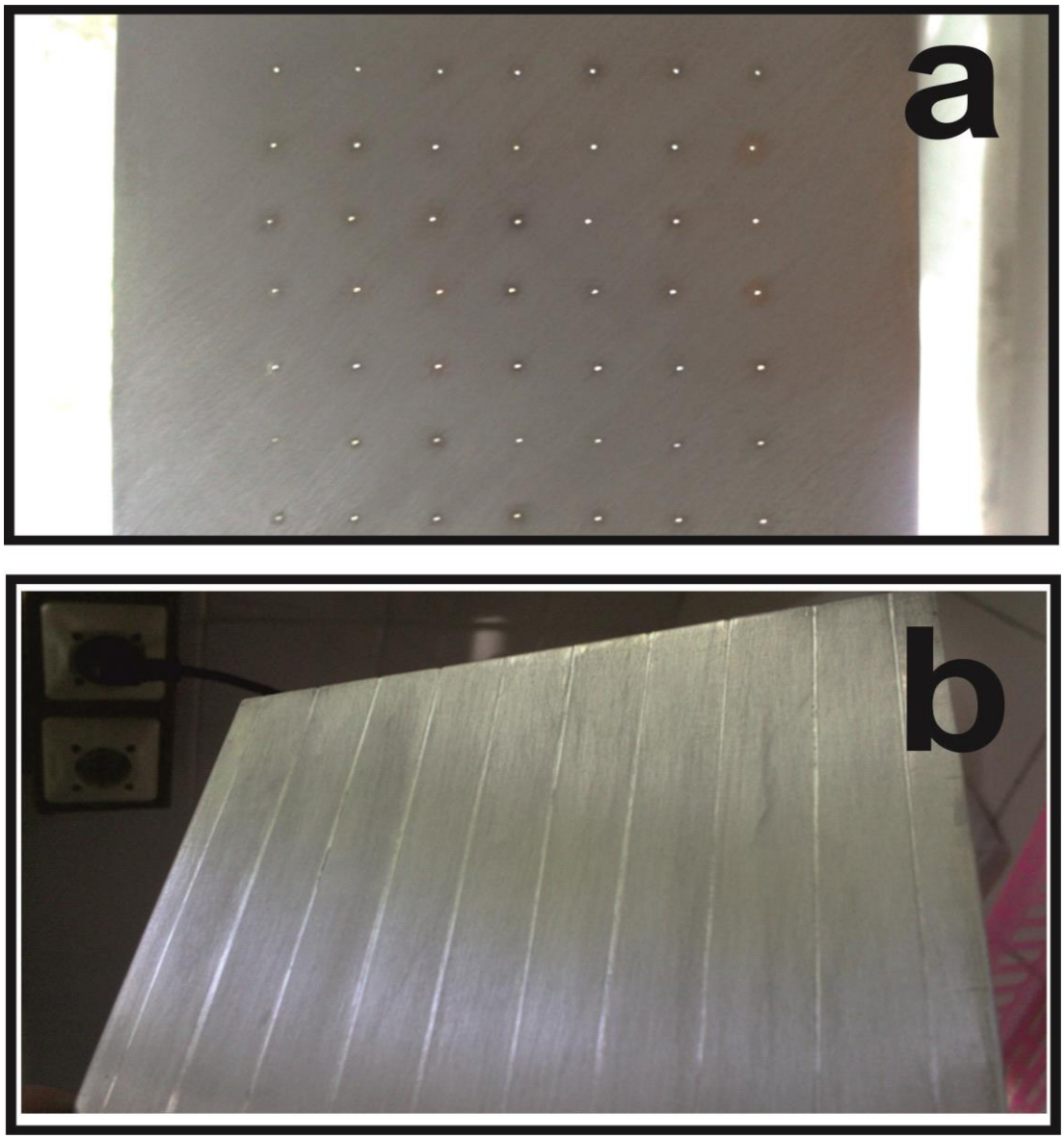

Figure 3.15 Hole (a) and groove (b) configurations on aluminum surfaces.0.2

Figure 3.16. X-ray photo of the fourth horizontal resin infusion sample containing holes.0.3

After completing the hole – groove modifications of the aluminum layers, abrasion with 1000 type sand paper was done. The other sand papers like 180/240/500 were used with the holes and grooves in order to minimize the mechanical deformation. Through the samples with no holes or grooves, 180 SB, 240 SB and 500 SB papers have been used before 1000 SB to create macro roughness.

After the completion of the abrasion with sand papers, all of the layers have been cleansed with acetone and the flatness of the parts have been controlled, and warped samples were stretched where necessary. After sand paper treatment, all of the aluminum layers have been cleaned with ultrasonic cleaner for ten minutes applying 50 Hz frequency at 50 °C. By using lint free tissue, cleaning and activating the surfaces with toluene followed ultrasonic cleaning.

Figure 3.17. Ultrasonic cleaning of aluminum substrates after sand paper abrasion.0.4

Silane preparation began after cleaning operation of the substrates. 95 vol% ethanol was mixed with 5 vol% pure water for half an hour. After sufficient mixing of these

two, to achieve the pH value between 4.5-5.5 interval acetic acid has been added. After stirring this solution for half an hour, 0.763 ml γ-glycidoxytrimethoxy silane was added and stirred for one and a half hour with magnetic stirrer.

After obtaining aluminum substrates as contaminant free as possible using ultrasonic cleaner and toluene for cleaning, silane treatment has been done on the aluminum surfaces with positive pressurized spraying machine with 0.2 Pa pressure using a nozzle. During silane treatment on the aluminum surfaces, pressure was always kept at the same level and the distance was arranged at 10±2 cm. Because multiple layer silane deposition will decrease the mechanical interlocking strength of the adhesion, the solution was sprayed over the substrate surface for only one time for both of the surfaces of the aluminum sheets. After silane treatment, all of the aluminum layers were kept at 110 °C for at least one hour. To hold the substrates at 110 °C is very critical just because over this temperature the silane burns out and below this temperature it does not make the bonding strong enough.

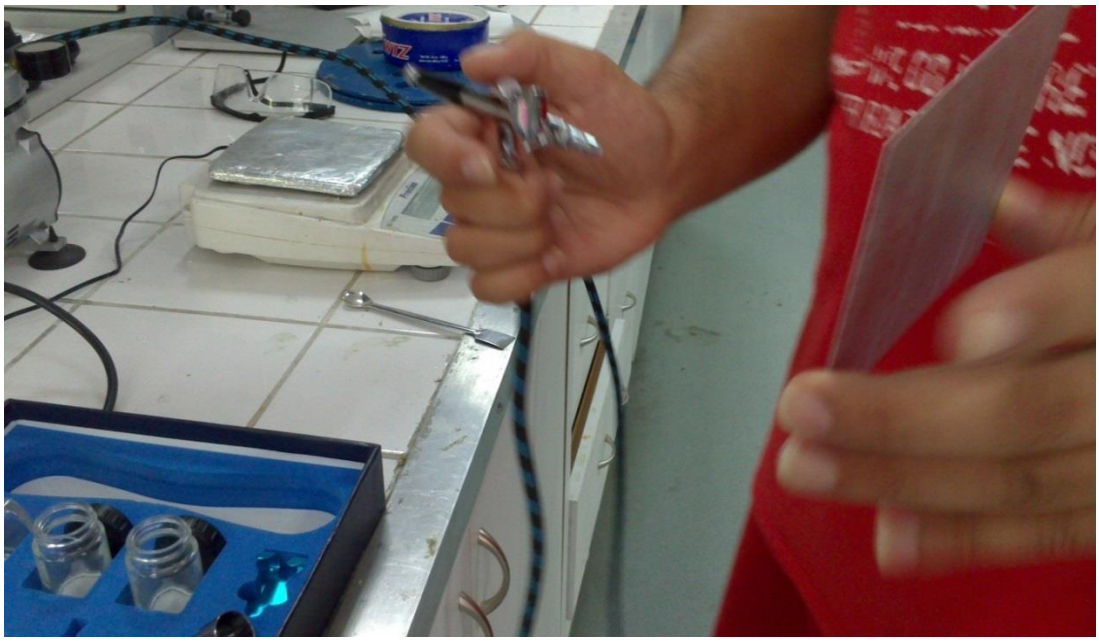

Figure 3.18. Silane treatment of aluminum substrates..0.5

After waiting for one hour at 110 °C aluminum sheets are ready to make adhesive bonding to the resin. After heat treatment in the furnace, flatness of the aluminum sheet has been checked again and stretched gently where needed. Arranging the 4 aluminum layers with 3 glass fiber layers between them finishes the aluminum preparation.

3.3.2. Resin Infusion Preparation

A thick glass plate containing bench has been produced in Ergül Makine/OSTİM facilities for only resin infusion experiments and applications in METE/METU facilities. To minimize the contamination and get the desired clean surface, the surface of the glass bench has been cleaned with pure water before ethanol and acetone cleansing. The other steps involved in the preparation for resin infusion are given below.

- The sealing tape has been placed on the bench according to the dimensions of the fiber metal laminate sample.
- The releasing paste has been smeared inside of the sealing tape area. After pasting the release agent, 10 minutes waiting time was applied.
- Vacuum bag and perforated laminate have been prepared according to the dimensions of the sample.
- Scratched hoses with two three gate junctions which fit to the dimensions were prepared.
- After arranging them, aluminum-fiber layers have been placed in the middle of the prepared site.
- Uniting the vacuum bag with the sealant tape and the three gate junctions has finalized the chamber of the resin infusion.

After tacking the resin and air hoses to the inlet and the outlet of the chamber respectively, preparations for the resin infusion process were complete. After taking the air out by vacuuming the chamber, closing the inlet and outlet openings of the chamber, the system was kept under this condition for nearly 20 minutes to see if there is any air leakage or not.

After seeing that there is no leakage, 40 g resins was mixed with 10 g hardener to prepare the two component resin. After stirring them slowly enough to avoid the resin from curing, they have been checked if the initial cloudy view has disappeared or not, where a clear mixture points out the readiness of the resin for the infusion process. When the resin has been let to go through the chamber, the chamber has been closed after seeing the exit of the resin from the outlet, and it was kept under sealed condition for at least 24 hour for curing.

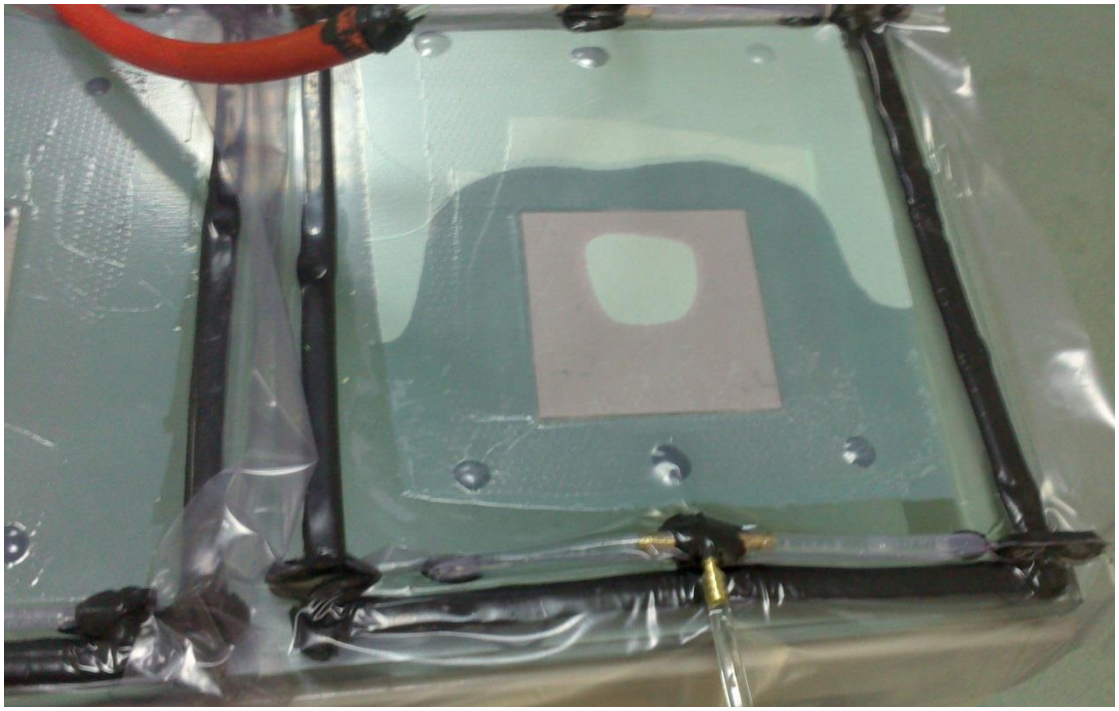

Figure 3.19. Progress of resin infusion.0.1

After taking the fiber metal laminate sample out of the infusion chamber, it has been placed in the furnace to post cure. Every sample of the fiber metal laminate composite has been kept at 80 °C for 4 hours or at 63 °C for at least 16 hours. After taking the samples out, their edges were abraded using Metkon Forcipol 2V grinder to get the proper cutting shape and geometry by removing the residual resin near the sample. After these steps the samples were ready to make the proper cutting of the three-point

bending test specimens. The samples have been sliced with Isomet 5000 micro cutter with dimensions 1 cm X 10 cm taking them from the mid sections of the samples.

Figure 3.20. Fiber metal laminate composites sliced with micro cutter.0.2

During cutting interval, the blade has released beach marks at the edge of the first sample. This edge has been created because of the layer differences of the composite structure, yet at the same time due to the damping of the motion of the blade between each layer. As a result, a piece of wooden block has been used with the holder of the micro cutter, and the formation of the beach marks has been suppressed.

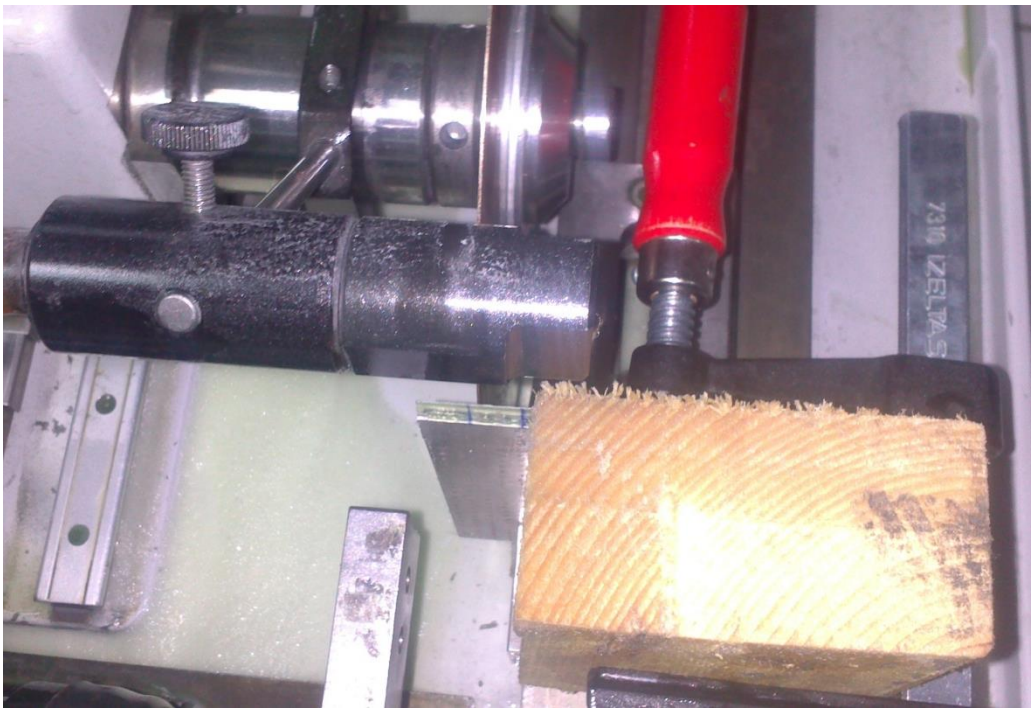

Figure 3.21. A wooden block has been used to prevent the damping of the blade.0.3

Inter laminar Shear Stress Test: The three point bending tests have been done on the samples which are listed below.

- Horizontal resin infusion for hole and 1.5 cm apart groove containing set with 1000 sand paper treatment, where the hole arrangement is given below in the Figure 3.22. (HV3)

Figure 3.22. Horizontal resin infusion sample containing holes as shown.0.4

- Horizontal resin infusion for hole and 1.5 cm apart groove containing set with 1000 sand paper treatment, where the hole arrangement is given below in the Figure 3.23. (HV2)

Figure 3.23. Horizontal resin infusion sample containing holes and 1.5 cm apart grooves.0.5

- Horizontal resin infusion for hole and 1.5 cm apart groove containing set with 1000 sand paper treatment, where the hole arrangement is given below in the figure. (HV1)
- Silane treated as received aluminum with prepreg.
- 180 sand paper treated aluminum with prepreg.
- 1000 sand paper treated aluminum with prepreg.
- Vertical resin infusion sample with 180 sand paper and silane treated aluminum.
- Vertical resin infusion sample with 1000 sand paper and silane treated aluminum.
- Trial sample for different wetting technique of aluminum surface.

The inter laminar shear stress values have been calculated following the three- point bending tests according to TSE EN 2563 using below given equation.

$$\tau = \frac{3.P}{4.b.h} \tag{40}$$

- τ =Inter laminar shear stress
- P=Actual force
- b=width of the sample
- h=height of the sample.

Different surface treatments and different composite production methods have been experienced during the study.

- Four types of horizontal resin infusion samples have been prepared. All of them have roughened with 1000 sand paper and silane treated. HVI-1 has got holes at every 1cms and at different points between 2nd and 3rd layers with grooves at every 1 cms. HVI-2 and HVI-3 have circlic pattern of the holes with 35 and 26 holes respectively and grooved at 1.5 cms and 2 cms respectively. HVI-4 sample has holes at every 1.5 cm and at different points between 2nd and 3rd layers with grooves at every 1.5 cms.

- Prepreg samples have been silane treated and 180 and 1000 sand papers have been except as received one.
- Vertical resin infusion samples have got no holes nor grooves and silane treated.

CHAPTER 4

RESULTS AND DISCUSSION

4.1. SEM Analysis of Samples

The change of the 1000 sand paper treated aluminum surface before and after silane treatment can be seen from the SEM images (Figure 4.1 and 4.2). There can be seen a contrast difference between the silane treated and only sand papered one.

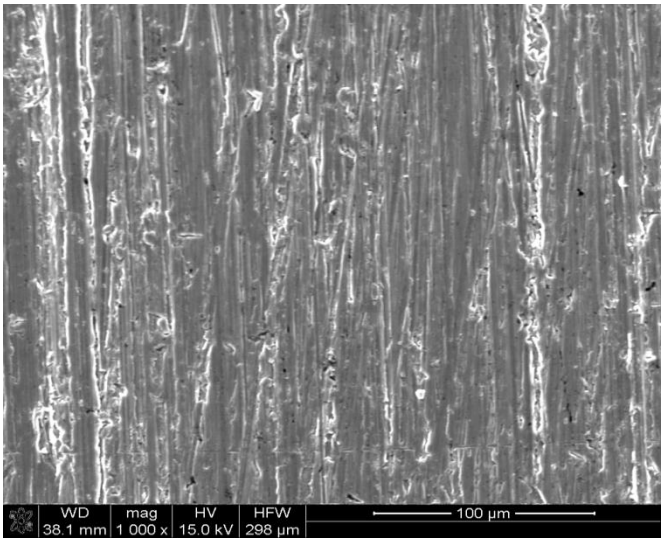

Figure 4.1. 1000 sand paper treated aluminum surface before silane treatment.0.1

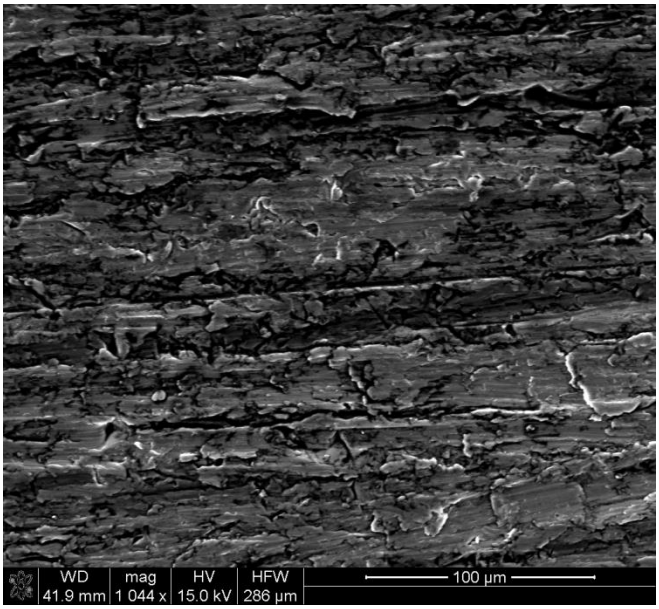

Figure 4.2. 1000 sand paper treated aluminum surface after silane treatment.0.2

4.2. Contact Angle Measurement

During manufacturing fiber metal composite, wetting is the most important phenomenon. The contact angle is the main issue to optimize the wetting of resin the aluminum 2024 T3 substrate. 9 different types of surface topography have been created on aluminum substrates with as-received aluminum, and contact angle measurements have been made in Atılım University facilities for these 9 cases. During measurements SEO 3000 contact angle measurement device has been used.

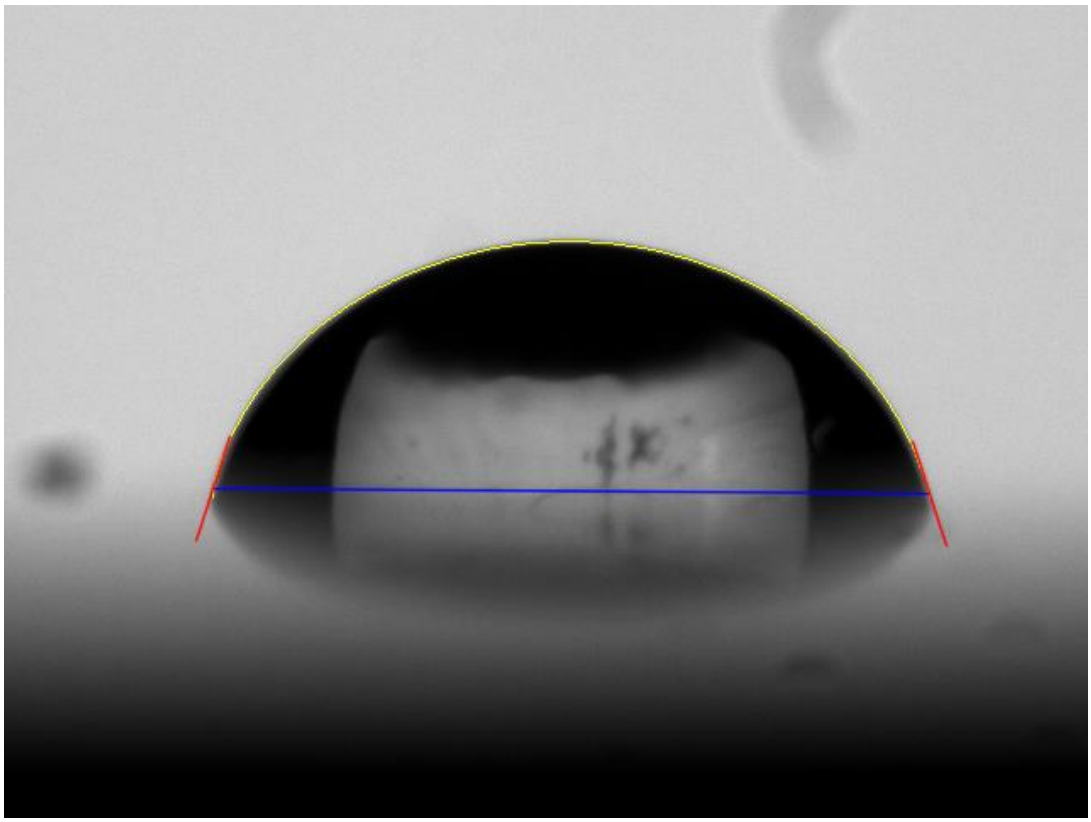

Figure 4.3. As-received aluminum surface contact angle measurement image.0.1

There is an injector on the device which spoils pure water drop on the substrates and a high resolution camera focused through the water droplet within the measurement set-up records an image. To catch the average contact angle 3 droplets have been spilled on each aluminum substrate. The results are given in Figure 4.4.

180, 240, 500 and 1000 grid sand papers have been used to modify the surfaces of the substrates. All of the roughening treatments were made linearly with papers except for the cyclic motions by 240 gridded sand paper. As can be seen on the graph, the cyclic motion resulted in the substrate with better/lower contact angle compared to the linear motion. However, as resin infusion takes place under negative pressure to make the triple line point travel successfully, linear pattern of regularly ground sand paper has been chosen.

The 1000 grid sand paper roughened surface topography gave the best/lowest contact angle results. Hole and groove containing samples of aluminum were roughened with

1000 sand paper, where minimum mechanical deformation against other sand papers and minimum contact angle results were obtained. Silane treated sample of the aluminum substrate has been roughened with 1000 sand paper because of the same reason.

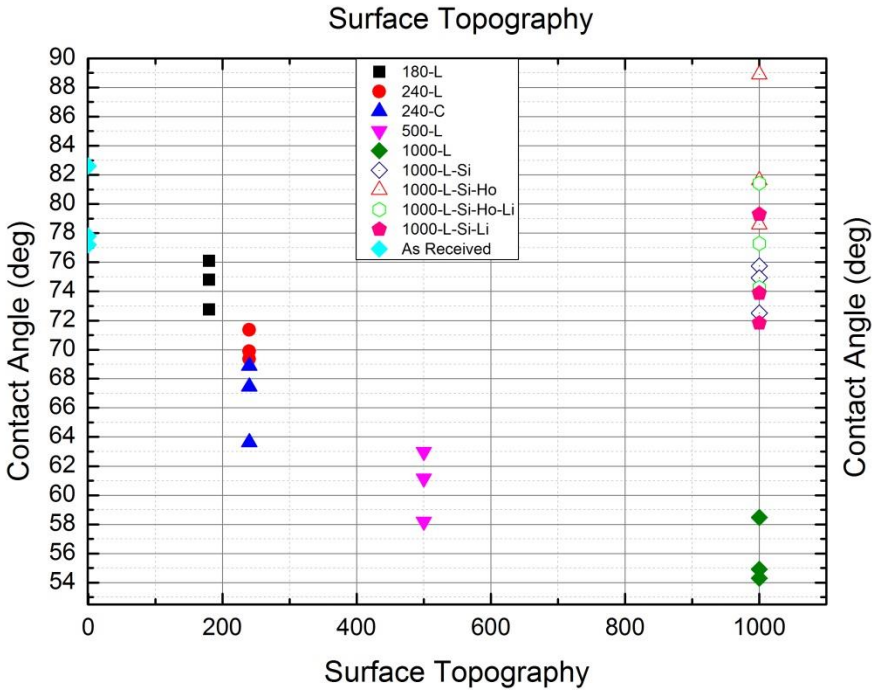

Figure 4.4. Aluminum contact angle measurements for different surface topographies.0.2

The 1000 sand paper did not give the maximum roughness but the best/lowest contact angles. For some other samples manufactured by prepreg, horizontal or vertical resin infusion processes different sand papers have been used.

4.3. Roughness Measurement

Roughening the surface increases the adhesion area. Because of this fact, aluminum substrate surfaces have been roughened using sand papers. Different average roughness values were created by sand papers having grid sized as shown in Figure 4.5. Although it has the optimum contact angle, 1000 sand papered surface (1000 SB) has got the lowest average roughness values among the others. However, after silane treatment (1000 SB+Si) the roughness increases to a value that is advantageous compared to only degreased aluminum surface topography.

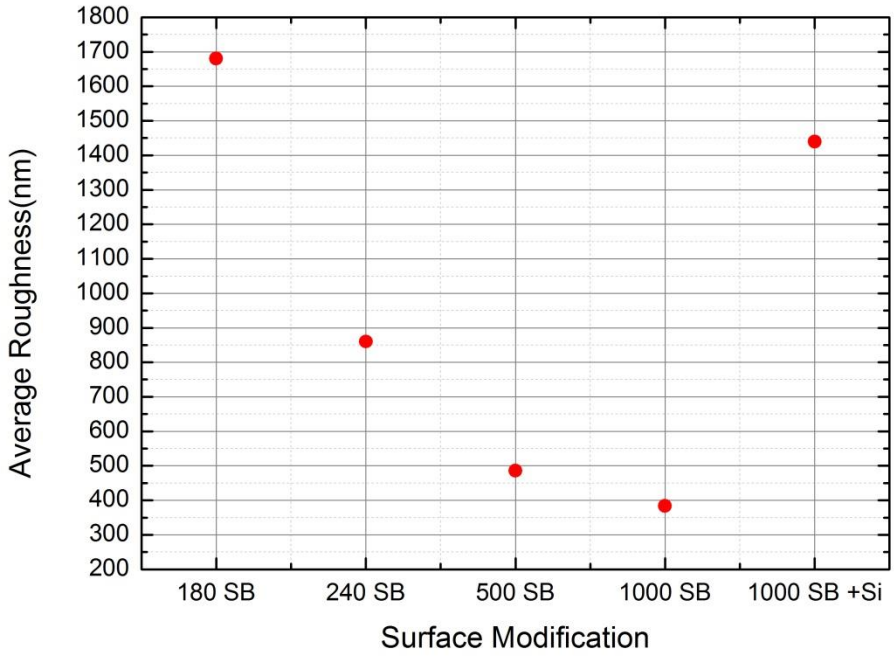

Figure 4.5. Average surface roughness values of different sand paper treatments. Figure 3

The values were measured in Micro Electro Mechanic Science/METU laboratories/facilities. Using the optical profilometer by Veeco all of the surfaces treated by varying methods were examined, and the light emitting performances of each of them gave the reflecting topography of the substrates. An example of the

measurements, for the 1000 sand paper and silane treated surface (1000 SB+Si) can be seen with a groove in the Figure 4.6 (a).

The optical profilometer provides average roughness values, as shown by red arrow in figure 4.7, yet also measures the maximum depth and height data of the surface topography simultaneously. At the same time from overall view of the other optical profilometer, the existing linearity of the sand paper treated surface lines can be observed by the special images which are called surface data as shown in the Figure 4.6 (b).

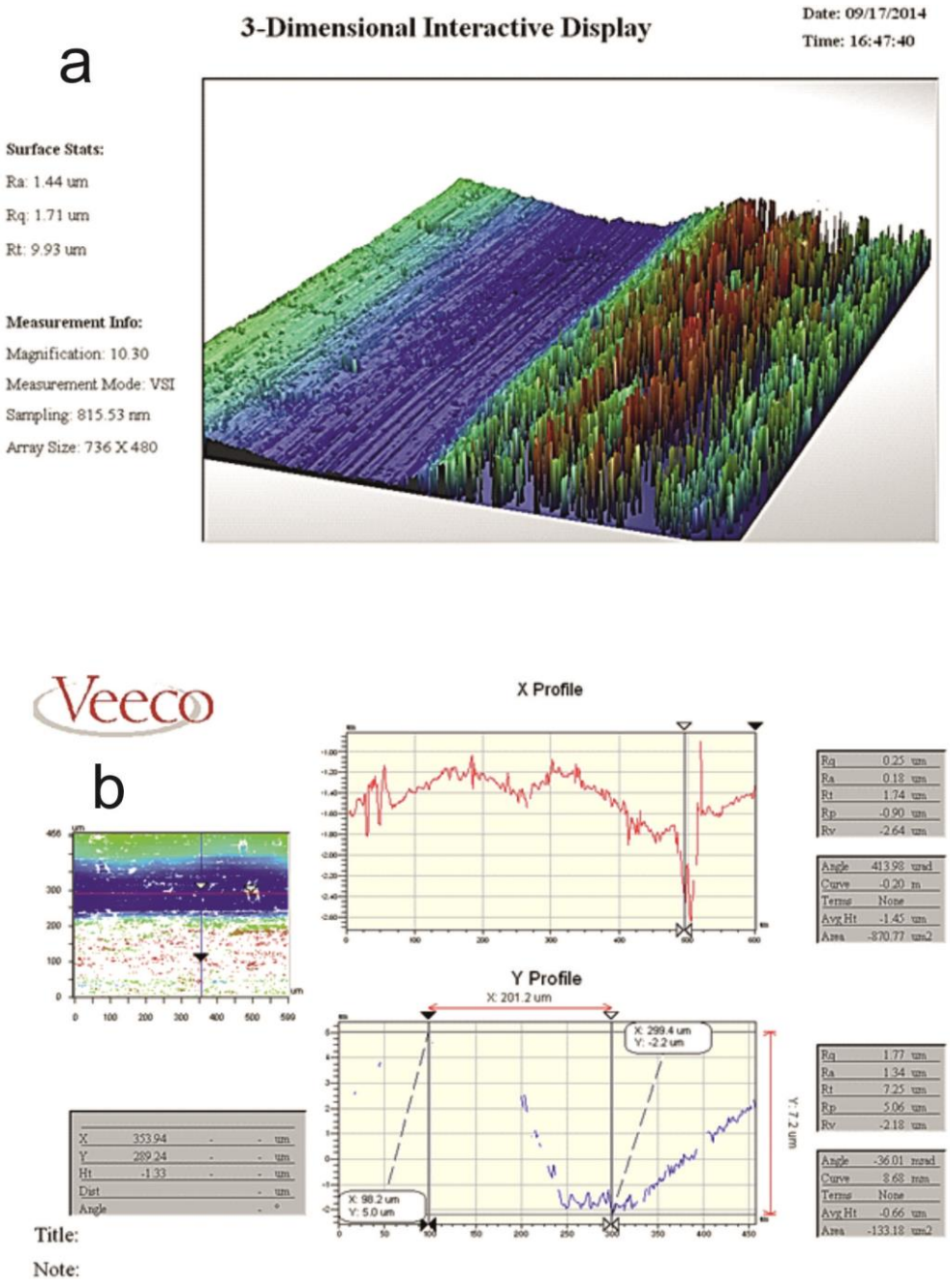

Figure 4.6. a) Surface topography of 1000 sand paper and silane treated substrate Optical profilometer display. b) Maximum height and depths of the substrate. surface.0.4

As can be seen in Figure 4.7, 180 sand paper treated surface has got better roughness according to 1000 sand paper treated surface yet the 180 paper treated one seems to lose the linearity of the lines where it has created relatively random grids. Scratches on the 1000 sand paper treated surface does not lose their linearity until the edge of the aluminum substrate.

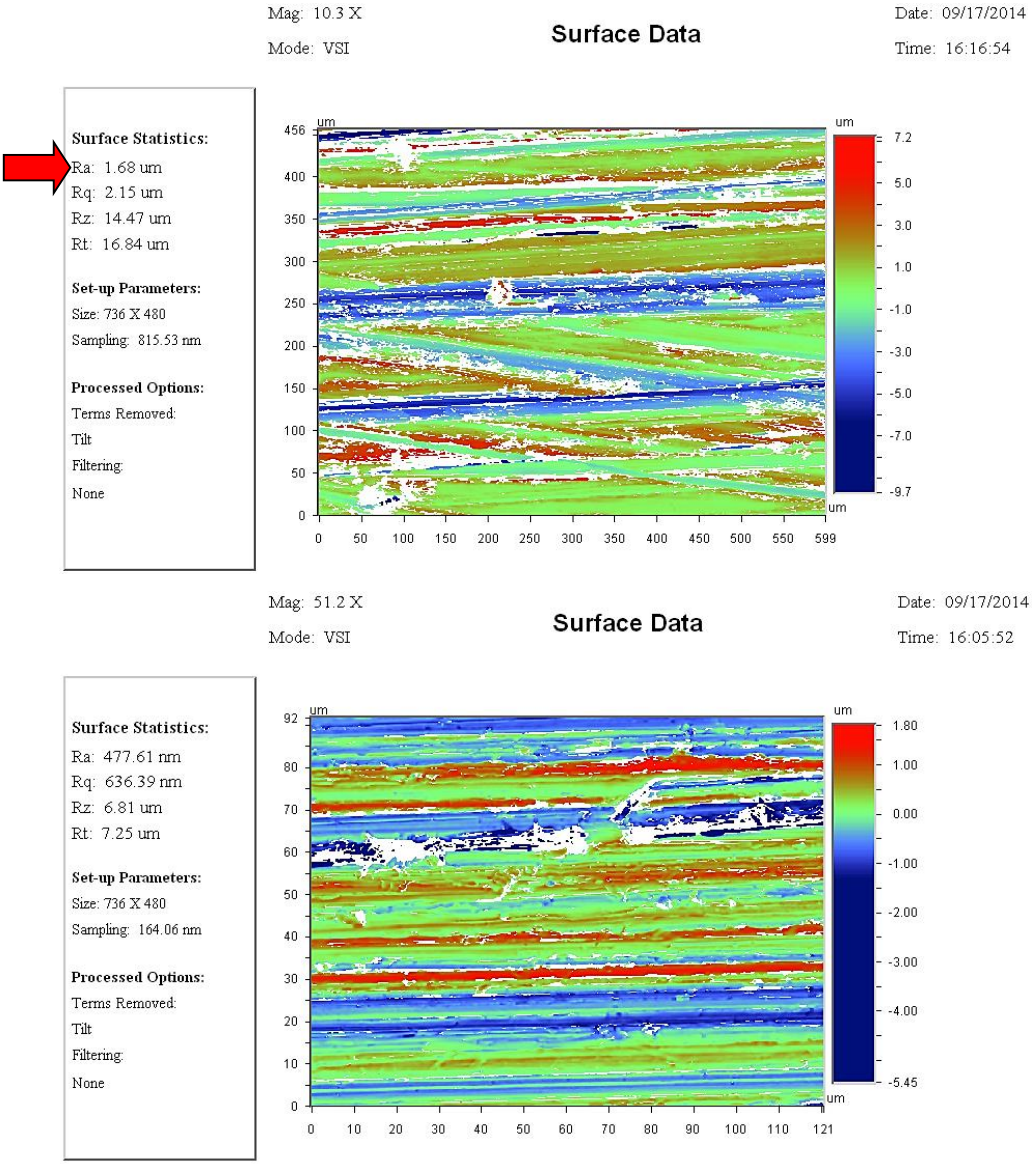

Figure 4.7. Surface data images of (a) 180 and (b) 1000 sand paper treated surfaces.

0.5

If it is assumed that the maximum value of height of roughness ~2.9 μm has been achieved on the 180 sand paper treated surface, the capillary pressure needed to overcome the trapped air in the so called regular little hills by the same roughness can be determined, as discussed in Chapter 2 in the wetting analysis. However, in the present case the negative pressure achieved in the mold during resin infusion is large enough to overcome that capillary pressure. So this is not a threat for resin infusion process unlike prepreg/autoclave considerations.

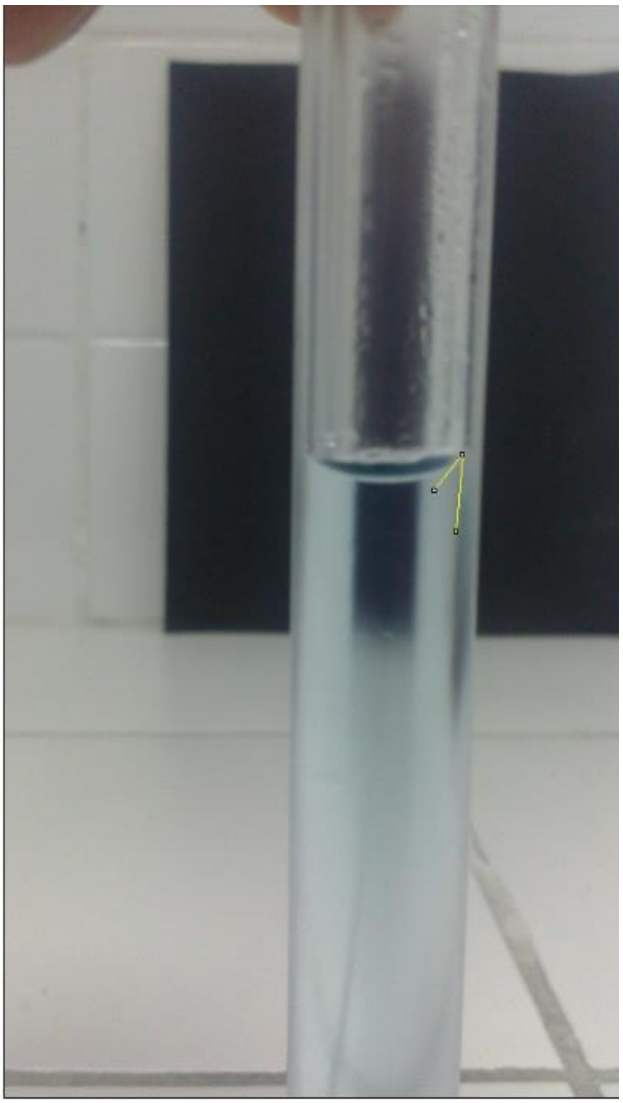

Figure 4.8. Surface tension measurement of the resin. Figure 6

Capillary rise of the resin in the hose is shown in figure 4.8. As can be seen in the reference [17];

$$\frac{2\gamma}{R} = \rho . g . h \qquad (41)$$

- γ=surface energy of the liquid
- ρ=density of the liquid=1,13 gr/cm^3
- h=height of the liquid in the hose=9,7 cm
- R=radius of the capillary rise

$$R = \frac{R1}{cos\theta} \qquad (42)$$

- θ=Angle of the capillary rise=32,54°
- R_1=inner radius of the hose=3,5 mm

R=8,1 mm

γ=8,71 N/m

Young's contact angle can be calculated by using equation (20) so;

$$\gamma cos\theta = \gamma_{SV} - \gamma_{SL} \qquad (43)$$

Using this analysis $\gamma_{SV} - \gamma_{SL}$ for different modified surfaces gives spreading coefficient, S;

$$S = \gamma_{SV} - \gamma_{SL} - \gamma \qquad (44)$$

$$S = \gamma cos\theta - \gamma \qquad (45)$$

In Table 4.1 spreading coefficients obtained by different surface modifications are given. If the spreading coefficient closes to zero and increases positively, it favors the spreading of the liquid, and hence wetting. As can be seen in Table 4.1 spreading coefficients of the linearly 180 sand paper treated surface (180 L) and the linearly 1000 sand paper and silane treated – grooved (1000 L+Si+Li) surface are the most favorable among the others. Linearly 1000 sand paper treated surface (1000 L) and linearly 240 sand paper treated surface (240 L) follow them. Linearly 1000 sand paper and silane treated – holed (1000L+Si+Ho) and linearly 1000 sand paper and silane treated (1000L+Si) surfaces are coming after them. Although it has good contact angle relative to some others, linearly 240 sand paper treated surface (240 L) gave the second worst result of spreading after linearly 1000 sand paper and silane treated – holed and grooved (1000L+Si+Ho+Li) one.

Even though some surface modifications including holes and grooves give possibility for better wetting through intra laminar pattern, they may not be preferred because they have the potential to decrease the mechanical strength of the composite.

Table 4.1. Calculated spreading coefficients of surfaces treated with different methods.

Modification Type	Average Contact Angle	cosθ	Spreading Coefficient
180 L	74,59≈75	0,26	-6,4454
240 L	70,18≈70	0,34	-5,7486
240 C	66,66≈67	0,39	-5,3131
500 L	60,78≈61	0,48	-4,5292
1000 L	55,89≈56	0,56	-3,8324
1000 L + Si	74,39≈74	0,28	-6,2712
1000 L + Si +Ho	83,04≈83	0,12	-7,6648
1000 L + Si +Ho + Li	77,66≈78	0,21	-6,8809
1000 L + Si + Li	75	0,26	-6,4454
As Received	79	0,19	-7,0551

According to Young's equation, roughness factor-$r=A/A_o$ can be found using as given in DeGennes' beautiful review[17];

$$\cos\theta_{rough}=r.\cos\theta_{smooth} \quad (46)$$

where θ_{rough} and θ_{smooth} are contact angles of the roughened and smooth surfaces respectively, and r is the roughness factor, in order to give idea about the increased area amount of the roughened surfaces.

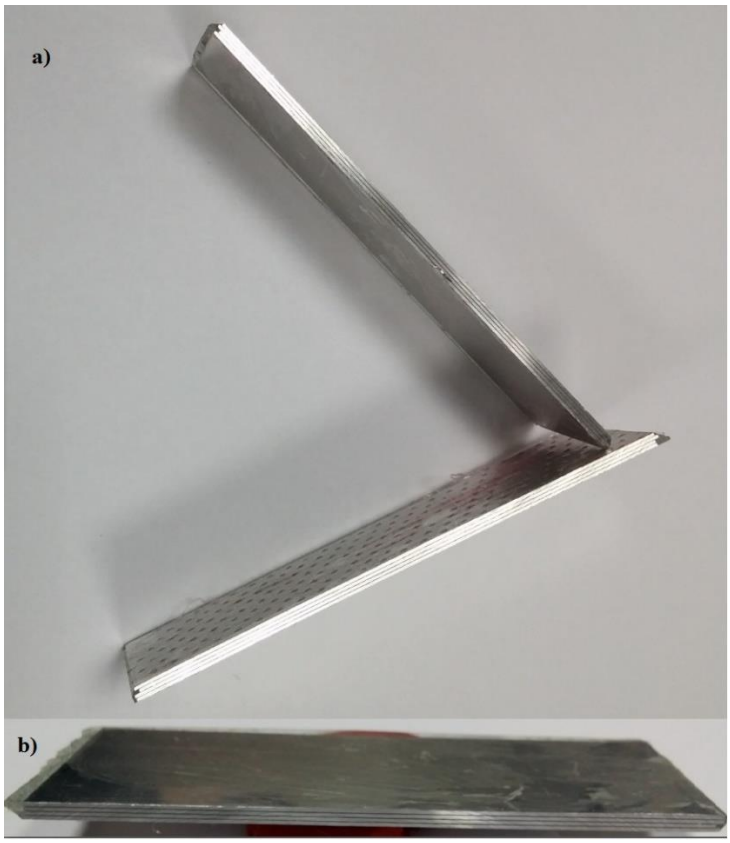

Figure 4.9. From a)Vertical and b)Horizontal views of fabricated samples **.Figure 0.7**

Table 4.2 Roughness Factor.

Modification Type	Contact Angle Rough	$\cos\theta_{smooth}$	Roughness Factor
180 L	74,59≈75	0,26	1,3684
240 L	70,18≈70	0,34	1,7894
240 C	66,66≈67	0,39	2,0526
500 L	60,78≈61	0,48	2,5263
1000 L	55,89≈56	0,56	2,9473
1000 L + Si	74,39≈74	0,28	1,4736
1000 L + Si +Ho	83,04≈83	0,12	0,6315
1000 L + Si +Ho + Li	77,66≈78	0,21	1,1052
1000 L + Si + Li	75	0,26	1,3684
As Received	79	0,19	1

Inter laminar shear stress values calculated by the data obtained using the three-point bending tests are given in Figure 4.8.

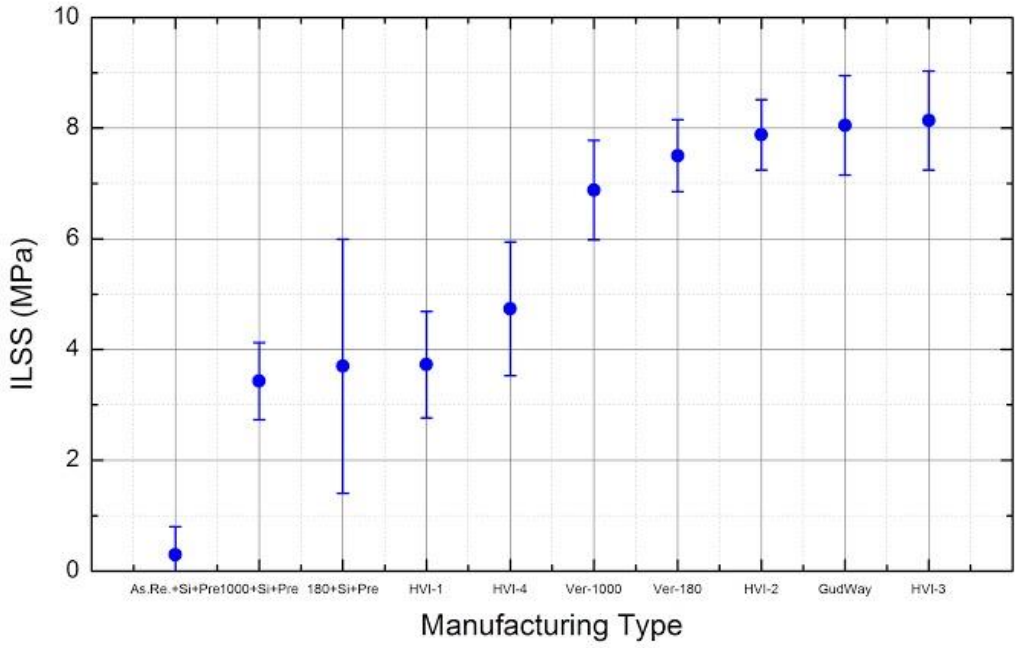

Figure 4.10. Inter laminar shear stress values of the fiber metal laminated composite samples.0.8

4 of the horizontal resin infusion samples representatively shown in Figure 4.10 contain fracture between the resin and the glass fiber. This shows that silane treatments has a positive effect yet because of the low inter laminar shear stress value the silane could not carry the adhesive load of the fiber metal laminated composite. The other four samples could not even be tested, because they have delaminated during cutting operation. Silane treated as received aluminum substrates which have been used during horizontally resin infusion sample preparation and with prepreg could not have been shown, either, because they have also delaminated during cutting operation.

Horizontal resin infusion samples revealed different results. Some samples fractured from the fiber-resin composite and some of the samples showed mixed fracture type. There is no consistency that could have created between them.
The HV-3 gave the highest inter laminar shear stress results and the best response to the splicing method optimization. It can be seen from Figure 4.11 that the line between the fiber-resin and the aluminum substrate is very thin and shows linearity through the line regularly. The splicing method application to this sample showed resistance against buckling or crack initiation in the interfaces with the optimum wetting (Figure 4.11). Figure.4.11 compares the separation intervals of the ref.[10] and ours.

Prepreg samples gave the lowest results as shown in the Figure 4.12. All of the sand paper-silane treated prepreg samples gave low inter laminar shear stress values which can be explained, as seen in Figure 4.12, by the huge space between the aluminum substrate and the prepreg. Therefore, it can be said that prepreg material does not give good results with silane treatment over the aluminum substrates.

In the aviation industry, GLARE® laminates have been fabricated with prepreg-autoclave manufacturing system. In this case, an adhesive primer, like BR 127, has been applied on the aluminum surfaces to increase the bonding strength with the prepreg. Prepregs have been used with other surface treatments in the literature like primer adhesive and anodizing which chase chemical etching. But in our case, the prepreg didn’t make desired bonding because the resin completed its’ reaction and couldn’t make the bond with silane.

These reasons make prepreg-autoclave manufacturing system unavailable for other surface treatments without primers. It has been mentioned that the prepreg-autoclave manufacturing system has got disadvantages being a long-batch process, using high electrical energy with high pressure and temperature within the autoclave and being rigid against complex shaping. Furthermore, the primer application increases the costs and the labor during fiber-metal laminated composite fabrication.

Vertical resin infusion samples showed relatively good values in terms of flexural and inter laminar shear stress. Although the values of the force during three-point bending stress test of vertical resin infusion samples, show consistency and give good results, the values are lower then the best horizontal resin infusion values. They showed very thin line of seperation between the fiber-resin composite and the aluminum substrate. However, one out of six samples showed delamination. Vertical resin infusion samples have the best average inter laminar shear stress values among the others fabricated by different systems.

When the stress-strain behavior given in Figure 4.14 and 4.15 are compared, it can be said that most of the fiber metal laminates fabricated in the scope of this study show stress-strain response close to those of Airbus Standart-GLARE® both in terms of strength and elongation.

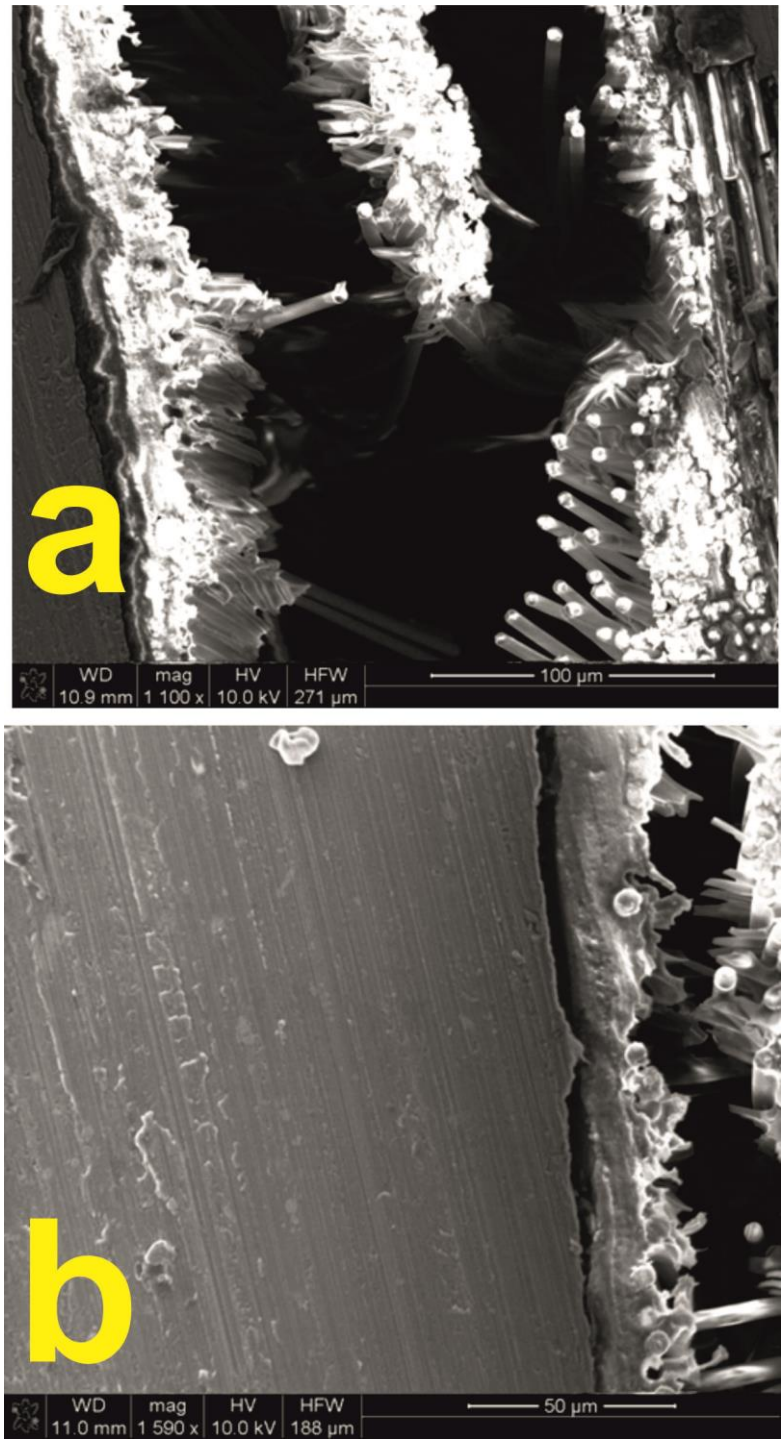

Figure 4.11. (a) Horizontal Resin Infusion-4. It can be seen that fracture occured in the fiber- resin part of the composite, not at the interface on the aluminum side. (b) The thin line observed shows the debonding between the aluminum and the fiber.0.9

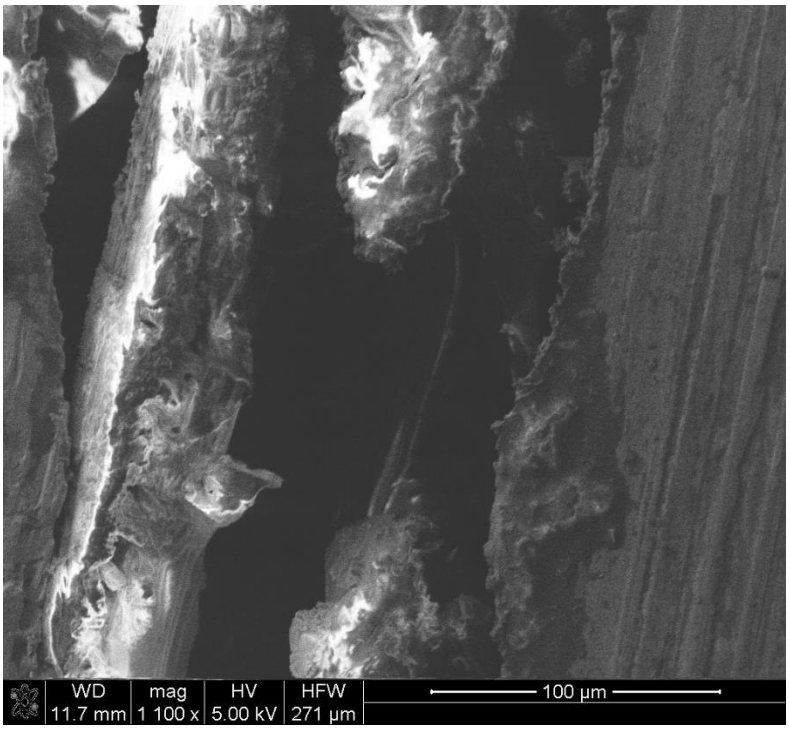

Figure 4.12. Horizontal resin infusion-HV-1 sample showing mixed type fracture, first from the fiber-resin composite than from the aluminum surface..0.10

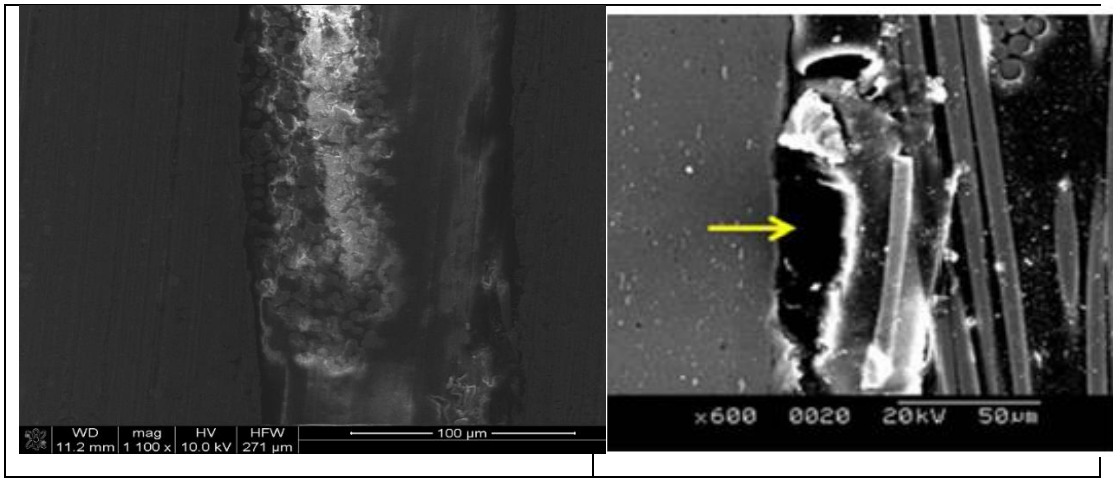

Figure 4.13. a) Horizontal resin infusion sample-HVI-7, showed cohesiveness of inter laminar shear stress against three-point bending test and did not show delamination. b) Debonding between aluminum and fibers in 220 sand blasting and phosphoric acid anodizing processed GLARE® [10]. 0.11

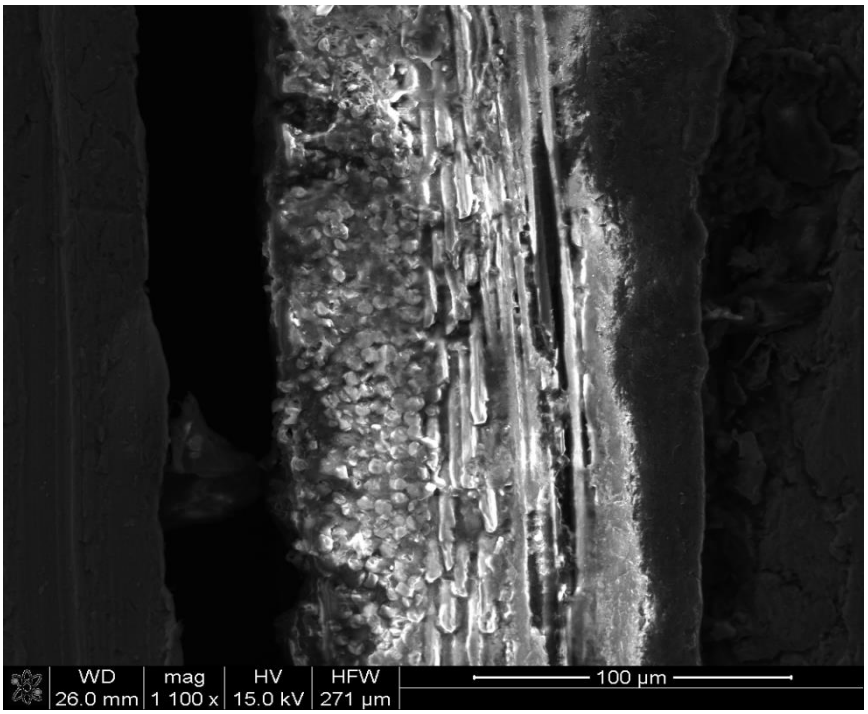

Figure 4.14. 1000 Sand Paper and Silane treated prepreg sample.0.12

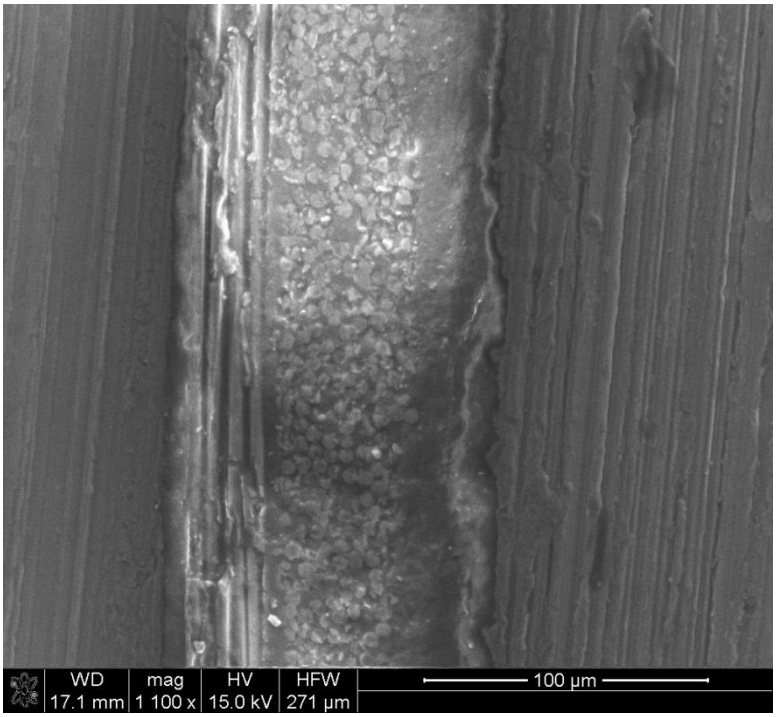

Figure 4.15. Vertical resin infusion sample-180 sand paper and silane treated.0.13

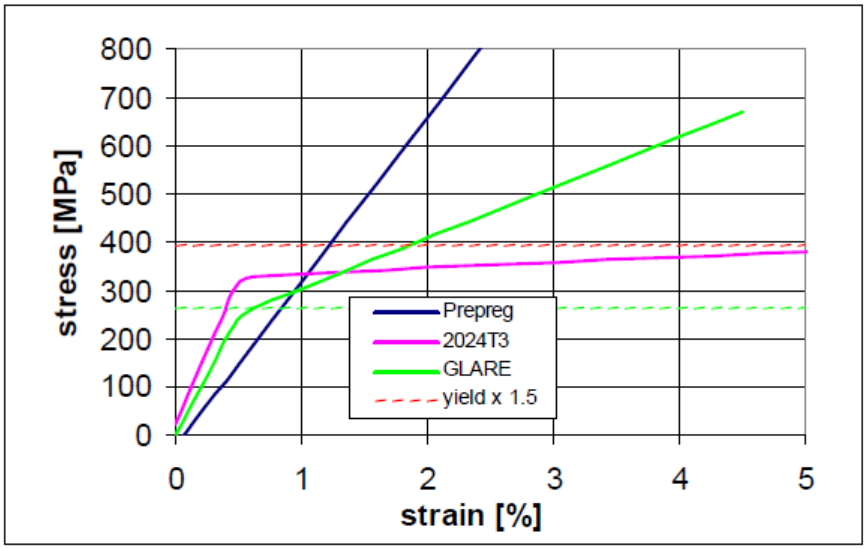

Figure 4.16. Stress-strain diagram of Airbus Standart-GLARE®. Area under the curve shows the energy absorption capability [7]. 0.14

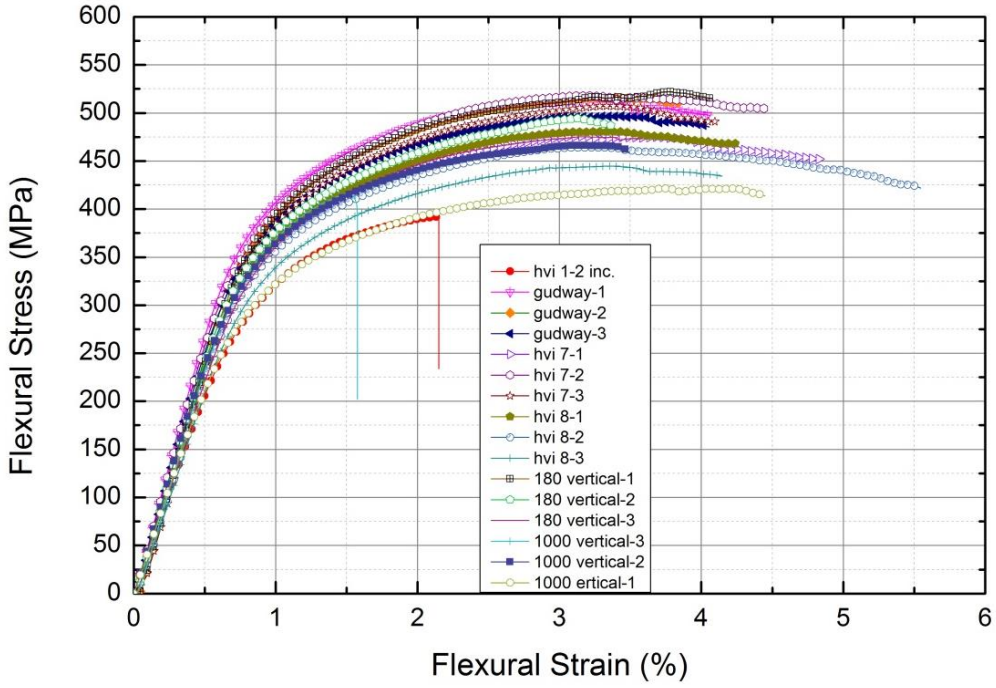

Figure 4.17. Stress – Strain diagrams of manufactured fiber metal laminated composites.0.15

When we compare the inter laminar shear stress results with the literature it can be seen that the inter laminar shear stress results extracted in this study are higher than the results as seen in the figure 4.18 from the ref.[60] , The strain rate in this study is 1 mm/minute.

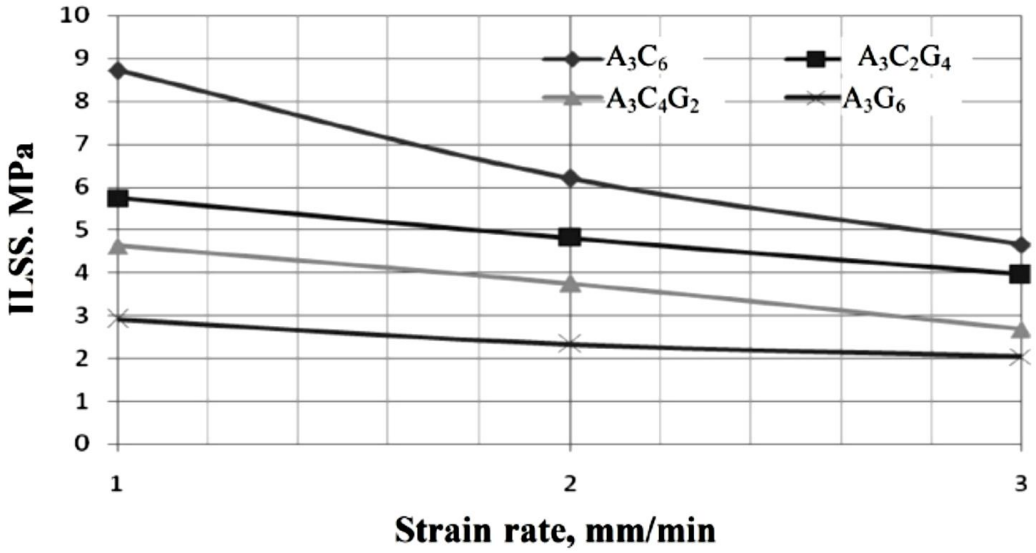

Figure.4.18. Variation of inter laminar shear strength as a function of strain rates for different fiber metal laminated structures.ref.[60]

The flexural stress results show and can be compared with aircraft company products and this manufacturing and surface treatment techniques can be used to fabricate fiber metal laminates for impact resistant and fatigue prone areas of the vessels. As assumed before the three point bending tests, it can be understood that the crack initiation and propagation started and created failure not between the metal substrates and the fiber-resin composites but between the fiber and the resin when the delamination or debonding have not been observed at the end of the tests.

CHAPTER 5

CONCLUSIONS

Resin infusion and tuned resin infusion processes will be the choice for the next generation fiber metal laminated composite manufacturing for different industries. As presented in this study, different types or modified kinds of silane may be used in the future to enhance the bonding of different fibers in laminated composites. The most important issue for the resin infusion process is create the know-how towards the appropriate use of the consumables involved.

Contamination is one of the main issues so manufacturing can be done in clean room facilities. Void content is the other main issue to be kept under control applying sensitive laboring.

From this study it is experienced that;

- Vertical resin infusion showed better consistency and can be tailored for fiber metal laminate manufacturing in the future by resin infusion technique.
- Fiber metal laminates can be manufactured by resin infusion method and horizontal resin infusion must be tailored and simulated for the efficiency and mechanical strength of the fiber metal laminates with the cyclic pattern of the holes and minimum grooves which give the best results according to splicing method.
- Silane treatment is an efficient method for surface adhesion.

- Sand paper treatment increases roughness and does not decrease mechanical strength of the aluminum so the treatments that have hazards can be eliminated by this simple method.

REFERENCES

1. Asundi, A., & Choi, A. Y. N. (1997). Materials Processing Technology Fiber Metal Laminates : An Advanced Material for Future Aircraft.

2. Cocchieri, E., Almeida, R., José, S., & Paulo, S. (2006). A Review on the Development and Properties of Continuous Fiber / epoxy / aluminum Hybrid Composites for Aircraft Structures 2 . The Production of Metal / laminate Hybrid Composites, 9(3), 247–256.

3. Wu, G., & Yang, J.-M. (2005). Analytical modelling and numerical simulation of the nonlinear deformation of hybrid fibre–metal laminates. Modelling and Simulation in Materials Science and Engineering, 13(3), 413–425. doi:10.1088/0965-0393/13/3/010

4. Cepeda-Jiménez, C. M., Alderliesten, R. C., Ruano, O. a., & Carreño, F. (2009). Damage tolerance assessment by bend and shear tests of two multilayer composites: Glass fibre reinforced metal laminate and aluminium roll-bonded laminate. Composites Science and Technology, 69(3-4), 343–348. doi:10.1016/j.compscitech.2008.10.010

5. Beumler, T.,(2004) A contribution to aircraft certification issues on strength properties in non-damaged and fatigue damaged GLARE® structures,Flying GLARE®.Retrieved November 2014 from file:///C:/Users/notebook/Desktop/ae_beumler_20040323.pdf.

6. Vermeeren, C. A. J. R., Kanter, J. L. C. G. D. E., Jagt, O. C. V. A. N. D. E. R., & Out, B. C. L. (2003). Glare® Design Aspects and Philosophies, 257–276.

7. Beumler, T., Starikov, R., Gennai, A., & Senatorova, O. (n.d.). Controlling the Damage with Fiber Metal Laminate Structures, First International Conference on Damage Tolerance of Aircraft Structures (2007).
8. Gan, Y. X. (2009). Effect of interface structure on mechanical properties of advanced composite materials. International Journal of Molecular Sciences, 10(12), 5115–34. doi:10.3390/ijms10125115

9. Vogelesang, L. B., & Vlot, A. (2000). Development of fibre metal laminates for advanced aerospace structures, 103, 3–7.

10. Park, S. Y., Choi, W. J., Choi, H. S., & Kwon, H. (2010). Effects of surface pre-treatment and void content on GLARE® laminate process characteristics. Journal of Materials Processing Technology, 210(8), 1008–1016. doi:10.1016/j.jmatprotec.2010.01.017

11. George, A. (2011). *Optimization of resin infusion processing for composite materials: Simulation and characterization strategies*. (Doctoral dissertation). Retrieved from http://elib.uni-stuttgart.de/opus/volltexte/2011/6263/pdf/GEORGE_PRINT.pdf

12. Lopes, C. S., Remmers, J. J. C., & Gürdal, Z. (2008a). Influence of Porosity on the Interlaminar Shear Strength of Fibre-Metal Laminates, 383, 35–52. doi:10.4028/www.scientific.net/KEM.383.35

13. Ragondet, A. . (n.d.).*Experimental characterization of the vacuum infusion process*. (Doctoral dissertation).

14. Critchlow, G. W., Yendall, K. a., Bahrani, D., Quinn, a., & Andrews, F. (2006). Strategies for the replacement of chromic acid anodising for the structural bonding of aluminium alloys. International Journal of Adhesion and Adhesives, 26(6), 419–453. doi:10.1016/j.ijadhadh.2005.07.001

15. Park, S. Y., Choi, W. J., Soap, H., Kwon, H., Kim, S. H., & City, K. (2010). Recent Trends in Surface Treatment Technologies for Airframe Adhesive Bonding Processing : A Review, (July 2012), 192–221.
16. Chamis, C. C., National aeronautics and space administration cleveland oh lewis research center, (1972). *Mechanics of load transfer at the fiber/matrix interface*. Retrieved from National Aeronautics and Space Administration Cleveland OH Lewis Research Center

17. deGennes, P.G., (1985).,Wetting: statics and dynamics, Review of modern physics57,827

18. June, J. W. M. B. (2013). 18.357 Interfacial Phenomena, Fall 2010

19. Duncan, B., Mera, R., Leatherdale, .D., Taylor, M., Musgroove, R.,(2005). Techniques for characterizing the wetting, coating and spreading of adhesives on surfaces, National Physics Laboratory

20. Bonn, D., Eggers, J., Indekeu, J., Meunier, J., & Rolley, E. (2009). Wetting and spreading. Reviews of Modern Physics, 81(2), 739–805. doi:10.1103/RevModPhys.81.739

21. .Branco, C. M., Ferreira, J. M., Faelt, P., & Richardson, M. O. W. (1996). A comparative study of the fatigue behaviour of GRP hand lay-up and pultruded phenolic composites, 18(4), 255–263.

22. Belingardi, G., Cavatorta, M. P., & Salvatore Paolino, D. (2008). Repeated impact response of hand lay-up and vacuum infusion thick glass reinforced laminates. International Journal of Impact Engineering, 35(7), 609–619. doi:10.1016/j.ijimpeng.2007.02.005

23. Gangloff, J. J., Simacek, P., Sinha, S., & Advani, S. G. (2014). A process model for the compaction and saturation of partially impregnated thermoset

prepreg tapes. Composites Part A: Applied Science and Manufacturing, 64, 234–244. doi:10.1016/j.compositesa.2014.05.010

24. Grunenfelder, L. K., & Nutt, S. R. (2010). Void formation in composite prepregs – Effect of dissolved moisture. Composites Science and Technology, 70(16), 2304–2309. doi:10.1016/j.compscitech.2010.09.009

25. Baumert, E. K., Johnson, W. S., Cano, R. J., Jensen, B. J., & Weiser, E. S. (n.d.). MECHANICAL EVALUATION OF NEW FIBER METAL LAMINATES MADE BY THE VARTM PROCESS.

26. Sala, G., & Camille, V. (1996). Advances in elastomeric tooling technology, 17(1), 33–42.

27. Morozov, E. V. (2006). The effect of filament-winding mosaic patterns on the strength of thin-walled composite shells. Composite Structures, 76(1-2), 123–129. doi:10.1016/j.compstruct.2006.06.018

28. Vargas Rojas, E., Chapelle, D., Perreux, D., Delobelle, B., & Thiebaud, F. (2014). Unified approach of filament winding applied to complex shape mandrels. Composite Structures, 116, 805–813. doi:10.1016/j.compstruct.2014.06.009

29. Wu, H. F., Wu,L.L., Slagter, J.W.,Verolme, L.J.,(1994). Use of rule of mixtures and metal volume fraction for mechanical property predictions of fibre-reinforced aluminium laminates Journal of Materials Science,29, 4583

.

30. Wu, G., & Yang, J. (2005). The Mechanical Behavior of GLARE® Laminates for Aircraft Structures,57, 72-79.

31. Kaufman,J.G. (1967). Fracture toughness of 7075-T6 and T651 sheet, plate and multilayered adhesive-bonded panles, journal of basic engineering, 89,503-507

32. Johnson, W.S., Rister, W.C., and Spamer, T. (1978). Spectrum crack growth in adhesively bonded structure ASME Journal of Engineering Materials and Technology, 100,57-63

33. Johnson, W.S. (1983).Damage tolerance evaluation of adhesively laminated titanium, ASME Journal of Material science and technology, vol.105,182-187.

34. Krishnakumar, S. (1994). Fiber Metal Laminates-the synthesis of metals and composite, Materials and manufacturing process, 9, 295-354.

35. Young, J.B., Landry, J.G.N., and Cavoulacos, V.N. (1994). Crack growth and residual strength characteristics of two grades of glass-reinforced aluminum 'GLARE ®, Composite Structures, 27,457-469.

36. Pitzer, C., Yang, J. M.,(2008).Hybrid Metal Laminate Manufacturing Planning Evaluation and assessment Retrieved November .2014 from http://www.pitzerconsulting.com/docs/FML-assessment_yang_pitzer_2009.pdf

37. Critchlow, G. W., & Brewis, D. M. (1996). Review of surface pretreatments for aluminum alloys, 16(4), 255–275.

38. Higgins, A. (2000). Adhesive bonding of aircraft structures , *20*(January), 367–376

39. Oosting, R. (1995).*Toward a new durable and environmentally compliant adhesive bonding process for aluminum alloys*. (Doctoral dissertation).,

40. Davis, G. D. and Venables, J. D. (2002). Surface Treatments of Metal Adherends,(Elsevier, Amsterdam,), 1st ed., Vol. 2, Ch. 21, pp. 947–1008.

41. Matz, C. W., Hilling, B., Kelm, W., and Kock, E. (September, 1996) Phosphoric Sulfuric Acid Anodizing (PSA) – A Heavy Metal Free Alternative for High Quality Surface Pretreatment of Aluminum, in: 83rd Meeting of the AGARD Structures and Materials Panel, Florence, Italy.

42. Johnsen, B.B. (2003). *Adhesive bonding of aluminum* (Doctoral dissertation)

43. Rider, A. N., & Arnott, D. R. (2000). Boiling water and silane pre-treatment of aluminium alloys for durable adhesive bonding, *20*

44. Abel, M.L., Watts, J.F.and Digby, R.P. (1998), The adsorption of alkoxysilanes on oxidised aluminium substrates,Int.J.Adhes.Adhes., 18, 179-192

45. . I, R. P., & Paekham, D. E. (1995). Pretreatment of aluminium : topography , surface chemistry and adhesive bond durability, *15*(2), 61–7

46. Mahesh, M., & A, S. K. (n.d.). Comparison Of Mechanical Properties For Aluminium Metal Laminates (GLARE®) Of Three Different Orientations Such As CSM , Woven Roving And 45 0 Stitched Mat, 9–13.

47. Hagenbeek, M., Hengel, C. V. A. N., Bosker, O. J., & Vermeeren, C. A. J. R. (2003). Static Properties of Fibre Metal Laminates, 207–222.

48. Chamis, C. C. (n.d.). MECHANICS OF LOAD TRANSFER AT THE FIBER / MATRIX INTERFACE.

49. Kashtalyan, M., & Soutis, C. (2007). Stiffness and fracture analysis of laminated composites with off-axis ply matrix cracking. Composites Part A:

Applied Science and Manufacturing, 38(4), 1262–1269. doi:10.1016/j.compositesa.2006.07.001

50. Airoldi, A., Vesco, M., Zwaag, S. Van Der, Baldi, A., Sala, G., & Masa, V. La. (n.d.). DAMAGE IN GLARE® LAMINATES UNDER INDENTATION LOADS : EXPERIMENTAL AND NUMERICAL RESULTS.

51. Nam, H. W. (2012). Design Factor Analysis of Fiber Metal Laminates under Concentrated Load by Using Design of Experiment. Applied Mechanics and Materials, 248, 167–172. doi:10.4028/www.scientific.net/AMM.248.167

52. Wang, W. D., Alderliesten, R. C., & Benedictus, R. (2014). On the Development of a Prediction Methodology for Crack Growth in Fibre Metal Laminates with MSD Scenario. Advanced Materials Research, 891-892, 1651–1656. doi:10.4028/www.scientific.net/AMR.891-892.1651

53. Fowkes, F.M.(1962), Determination of Interfacial Tensions, Contact Angles and Dispersion Forces in Surfaces by Assuming Additivty of Intermolecular Interactions in Surfaces,J.Phys.Chem.66,382

54. Packham, D. . (2003). Surface energy, surface topography and adhesion. *International Journal of Adhesion and Adhesives*, *23*(6), 437–448. doi:10.1016/S0143-7496(03)00068-X

55. Shafrin, E.G., Zisman,W.A.(1964) Contact angle, wettability and adhesion, Advances in Chemistry Series, 43, 145–157.

56. .Quere, D.(2002) Rough ideas on wetting, Physica A, 313,32-42

57. Bico, J.,Thiele, U., & Quere, D. (2002). Wetting of textured surfaces, *206*, 41–46.

58. Elizabeth, B.,Dussan ,V., B., Davis, S.H., (1974). On the motion of a fluid-fluid interface along a solid surface, Journal of Fluid Mechanics,65,71-95.

59. , E., Prost, J., & Bouletl, C. (1982). Attention aux tensions superficielles , *159*

60. Investigation of tensile and bending behavior of aluminum based hybrid fiber metal laminates by, G.R. Rajkumar, M.Krishna, H.N.Narasimhamurthy, KEshavamurthy, Y.C., J.R.Nataraj.